PD-1 blockade following isolated limb perfusion with vaccinia virus prevents local and distant relapse of soft-tissue sarcoma

Authors: Henry G Smith[1,2], David Mansfield[1], Victoria Roulstone[1], Joan N Kyula-Currie[1], Martin McLaughlin[1], Radhika Patel[3], Katharina Bergerhoff[1], James T Paget[1], Magnus T Dillon[1], Aadil A Khan[1], Alan A Melcher[4], Khin Thway[2], Kevin J Harrington[1*†], Andrew J Hayes[2*].

Affiliations:

[1]Targeted Therapy Team, The Institute of Cancer Research, London, UK.

[2]The Sarcoma Unit, Department of Academic Surgery, The Royal Marsden Hospital NHS Foundation Trust, London, UK

[3]Flow Cytometry and Light Microscopy Facility, The Institute of Cancer Research, London, UK.

[4]Translational Immunotherapy Team, The Institute of Cancer Research, London, UK.

* Joint senior authors

† Correspondence to Prof. K. J. Harrington, Targeted Therapy Team, The Institute of Cancer Research, London, UK (Kevin.Harrington@icr.ac.uk).

The authors declare no potential conflicts of interest.

Running title: Viral ILP augments PD-1 blockade for durable cure in sarcoma

Translational relevance: Currently available treatments to treat or prevent metastatic sarcoma are limited. PD-1 blockade has minimal efficacy in sarcoma, with these tumours considered immunologically cold. Here we demonstrate that the response to PD-1 inhibition can be dramatically enhanced following prior treatment with a vaccinia virus delivered alongside bio-chemotherapy in ILP in a model of extremity soft-tissue sarcoma. Vaccinia virus induced markers of immunogenic cell death in several sarcoma cell lines and promoted the infiltration and activation of cytotoxic T cells and dendritic cells when combined with PD-1 blockade *in vivo*. When performed as a neoadjuvant treatment prior to surgery and radiotherapy, viral ILP and PD-1 blockade secured durable cure of local and distant disease, transforming ILP from a locoregional treatment into a curative systemic therapy for sarcoma. Our therapeutic protocol may be directly translated into clinical practice and could represent an effective local and systemic therapy for extremity soft-tissue sarcoma.

Abstract:

Purpose: The prevention and treatment of metastatic sarcoma are areas of significant unmet need. Immune checkpoint inhibitor monotherapy has shown little activity in sarcoma and there is great interest in identifying novel treatment combinations that may augment responses. *In vitro* and *in vivo*, we investigated the potential for an oncolytic vaccinia virus (GLV-1h68) delivered using isolated limb perfusion (ILP) to promote anti-tumour immune responses and augment response to PD-1 blockade in sarcoma.

Experimental design: In an established animal model of extremity sarcoma, we evaluated the potential of locoregional delivery of a vaccinia virus (GLV-1h68) alongside bio-chemotherapy (melphalan/TNFα) in ILP. Complimentary *in vitro* assays for markers of immunogenic cell death were performed in sarcoma cell lines.

Results: PD-1 monotherapy had minimal efficacy *in vivo*, mimicking the clinical scenario. Pre-treatment with GLV-1h68 delivered by ILP (viral ILP) significantly improved responses. Furthermore, when performed prior to surgery and radiotherapy, viral ILP and PD-1 blockade prevented both local and distant relapse, curing a previously treatment-refractory model. Enhanced therapy was associated with marked modulation of the tumour microenvironment, with an increase in the number and penetrance of intratumoural $CD8^+$ T cells and expansion and activation of dendritic cells. GLV-1h68 was capable of inducing markers of immunogenic cell death in human sarcoma cell lines.

Conclusions: Viral ILP augments the response to PD-1 blockade, transforming this locoregional therapy into a potentially effective systemic treatment for sarcoma and warrants translational evaluation.

Introduction

Soft-tissue sarcomas are a group of rare, heterogeneous tumours derived from mesenchymal tissues, with an annual incidence of approximately 5/100,000 persons (*1*). The most commonly affected sites are the extremities, accounting for approximately 40% of all cases (*2*). Limb conserving surgery and adjuvant radiotherapy is highly effective in securing long term control of the primary tumour (*3*). Although such treatment secures local control in the limb in more than 85-90% of patients, rates of systemic relapse are high, approaching 30% at 5 years for all patients with sarcoma (*4, 5*). The evidence base that adjuvant chemotherapy can lessen the risk of metastatic sarcoma is not strong (*6, 7*). Once metastatic disease is established, systemic cytotoxic chemotherapies are relatively ineffective, with patients having a median survival of only 12 months (*8*). Therefore, the development of new strategies for the prevention and/or treatment of metastatic sarcoma is an area of great clinical importance.

Immunotherapies, in particular immune checkpoint inhibitors, have markedly improved the prognosis of patients with historically poor-prognosis cancers, such as metastatic melanoma (*9-11*). However, evidence from early clinical studies suggests that these agents have limited efficacy in either soft-tissue or bone sarcomas (*12, 13*). Determinants of response to immune checkpoint blockade in other pathologies have been defined, with such factors as tumour mutational burden, $CD8^+$ T cell infiltration, upregulation of interferon gamma-related genes and tumour cell expression of immune checkpoint ligands found to be associated with greater activity (*14-18*). By combining immune checkpoint inhibitors with other immune-activating cancer therapies, it is thought that it may be possible to cause tumours to display some of these characteristics, increasing their sensitivity to immune checkpoint blockade. Oncolytic viruses

represent attractive candidates for such combinations, since they are increasingly recognised as immunotherapies in their own right and have highly favourable toxicity profiles (*19*).

To date, the only route of viral delivery shown to be clinically effective is intra-tumoural injection, with the modified herpes simplex type I virus talimogene laherparepvec (Imlygic, Amgen) now licensed for patients with stage IIIB-IV melanoma (*20*). However, the optimal route for viral delivery to soft tissue sarcoma remains to be defined. Intra-tumoural delivery may be less efficacious than in melanoma due to the size and depth of these tumours. Systemic viral delivery would be ideal, allowing multiple tumour sites to be treated simultaneously but this approach is yet to demonstrate clinical efficacy. This may be due to eradication or sequestration of circulating virus by antiviral defences, preventing the delivery of sufficiently high viral titres to the tumour. Nevertheless, intravenous delivery of several strains of virus has demonstrated tropism for tumours, with mounting evidence that virus delivered in this fashion can promote a more inflamed tumour microenvironment, which may render the tumour more susceptible to subsequent immune checkpoint blockade (*21-24*).

We have previously shown that locoregional delivery of virus by Isolated Limb Perfusion (ILP) to be an effective alternative to systemic administration (*25, 26*). ILP is the locoregional delivery of chemotherapy, usually melphalan and tumour necrosis factor-α (TNFα), to a tumour-bearing limb that has been surgically isolated from the systemic circulation. Not only does ILP allow the delivery of melphalan at doses many times greater than could be tolerated systemically, it also allows the safe delivery of intravascular TNFα, whose vasoactive effects enhance the permeability of the tumour's microvasculature, thereby increasing the penetrance of melphalan

within the tumour (*27*). ILP has a well-established role in the management of locally advanced extremity sarcomas, either as a stand-alone treatment to avoid amputation or a neoadjuvant therapy to facilitate function-preserving resections (*28, 29*).

Locoregional delivery of virus by ILP has theoretical benefits over intratumoural injection or systemic delivery. As well as targeting the delivery of high viral titres to the tumour-bearing limb, isolation of virus within the limb circulation prevents first pass metabolism in the liver and viral sequestration within the reticuloendothelial system. Furthermore, the vasoactive effects of TNFα may increase viral penetrance of the tumour. Previous work by our team, using an animal model of extremity sarcoma and a modified vaccinia virus (GLV-1h68), found that the addition of GLV-1h68 to standard-of-care ILP delayed tumour growth and prolonged survival (*25*). However, when this combination was used neoadjuvantly prior to surgery and radiotherapy, viral ILP was insufficient to prevent the development of metastatic disease even though local control could be achieved (*26*).

Here we demonstrate that the delivery of GLV-1h68 delivered by ILP substantially improves response to subsequent PD-1 blockade in a rodent model of high-grade extremity sarcoma. The combination of a viral ILP with anti-PD-1 antibodies led to dramatic alterations in the sarcoma tumour microenvironment (TME), with the expansion of both effector T cells and dendritic cells. When combined with surgical resection and radiotherapy, this combination immunotherapy achieved durable cure of both local and distant disease in a previously treatment-refractory model.

Materials and Methods

Study design. Using an immune-competent, orthotopic and metastatic animal model of ESTS we characterized the efficacy of anti-PD-1 antibody monotherapy. We assessed the therapeutic benefit of combining anti-PD-1 blockade with the locoregional delivery by ILP of a modified vaccinia virus alongside standard biochemotherapy. The ability of this combination therapy to control local and systemic disease relapse was evaluated in both palliative and neoadjuvant protocols. To elucidate the mechanism responsible for enhanced therapy, we characterized effects of treatment on the tumour microenvironment in our *in vivo* model using flow cytometry, immunohistochemistry and RNAseq. We also assessed the production of recognized markers of immunogenic cell death in rodent and human sarcoma cell lines *in vitro*. A single investigator performed all the surgical procedures and adjuvant irradiations. Sample sizes were determined using a power calculation based on detecting a 20% difference between control and treated cohorts.

Cell lines and culture. BN175, HT1080 and SW872 cell lines were passaged in Dulbecco's Modified Eagle's Medium (DMEM), supplemented with 5% heat-inactivated foetal bovine serum (FBS), 2.5% L-glutamine and 1% penicillin/streptomycin and maintained at 37°C and 10% CO_2.

Therapeutic agents. GLV-1h68 was produced and provided by Genelux Corporation (San Diego, CA, USA). GLV-1h68 is an attenuated vaccinia virus and was constructed as previously described (*53*). Melphalan (Alkeran) was purchased from Laboratoires Genopharm, France. Recombinant human tumour necrosis factor alpha was purchased from First Link Ltd

(Birmingham, UK). Anti-PD-1 antibody (clone J43) and the relevant isotype (Armenian Hamster IgG) were purchased from 2BScientific (Upper Heyford, UK).

In vitro *validation of anti-PD-1 antibody cross-reactivity*. Recombinant rat PD-1 protein was purchased from Sino Biological (Wayne, PA, USA). After reconstitution, the recombinant protein was conjugated to flow cytometry beads using the Functional Bead Conjugation kit from Becton Dickinson (Wokingham, UK). Samples were stained with the J43 anti-PD-1 antibody and the relevant isotype control then with an Alexa Fluor 488 fluorescent secondary antibody (Thermo Fisher Scientific, Hemel Hempstead, UK) and assessed using flow cytometry.

In vivo *studies.* Inbred, male Brown Norway rats weighing between 225-275 g were obtained from Envigo (Huntingdon, UK). Tumours were established by injecting 1 x 10^7 BN175 cells subcutaneously into the left biceps femoris muscle. For anti-PD-1 monotherapy, treatment started 6 days after tumour implantation, with 3 doses of 200 □g of anti-PD-1 or isotype antibody delivered by intraperitoneal injection at 48-hour intervals. ILP was performed as previously described and combined with anti-PD-1 antibodies/isotype controls in palliative (Figure 2A) and neoadjuvant (Figure 3A) protocols (*25*). An Institutional Animal Care and Use Committee (IACUC) approved the *in vivo* experiments.

Immunogenic cell death assays. For ATP release, cells were plated at 5 x 10^4 cells/well, incubated overnight and treated with the indicated therapeutics. At the relevant time points, 200 □l of medium were collected and centrifuged to remove cellular debris. Fifty □l of Cell Titre Glo (Promega, Madison, WI, USA) were then added and luminescence immediately quantified

with a SpectraMax 384 plate reader (Molecular Devices, Berkshire, UK). For HMGB1 secretion, 1 x 10^6 cells/well were incubated overnight and treated with the indicated therapeutics. Culture supernatants were collected after 72 hours and secreted HMGB1 quantified by ELISA (IBL International, Hamburg, Germany). For cell surface calreticulin (CRT) expression, cells were plated at 3 x 10^5 cells/well, incubated overnight and treated with the indicated therapeutics. After 24 hours, cells were collected and stained with a primary anti-CRT antibody (Thermo Fisher Scientific) and Fixable viability dye-eFluor 780 (Thermo Fisher Scientific). CRT expression was then analysed with flow cytometry, with dead cells excluded from analysis.

Flow cytometry. For *in vitro* analysis of PD-L1 expression, cells were stained with a PD-L1 primary antibody (Proteintech, Manchester, UK) and an Alexa Fluor 488 secondary (Thermo Fisher Scientific). For *in vivo* analysis of tumours and tumour-draining lymph nodes, tissues were harvested from tumour-bearing Brown Norway rats. Both tissues were stained with two separate panels. Panel 1 comprised CD3-APC, CD4-PE, Granzyme B-Pacific Blue (Biolegend, San Diego, CA, USA), CD8-PE Cy7, Foxp3-Alexa Fluor 700 and Fixable viability dye-eFluor 780 (Thermo Fisher Scientific). Panel 2 comprised CD3-APC, CD161-PE, Granzyme B-Pacific Blue (Biolegend) and Fixable viability dye-eFluor 780 (Thermo Fisher Scientific).

Immunohistochemistry. Analyses were performed on formalin-fixed paraffin-embedded (FFPE) sections. Primary antibodies specific for rat PD-L1 were sourced from Proteintech and for rat CD3 and CD8 were sourced from Thermo Fisher Scientific. Digital images of the stained slides were obtained using the Nanozoomer-XR platform (Hamamatsu Photonics, Welwyn Garden City, UK). For the comparison of immune infiltrates in tumours at the humane endpoint, 10

fields of view at 20X magnification were randomly selected from 6 samples in each cohort. For the analysis of CD8 topography, 5 fields of view at 20X magnification were randomly selected from both the invasive margin and the tumour parenchyma, respectively, from 6 samples in each cohort. Staining was quantified using Cell Profiler software (*54*).

RNA sequencing and bioinformatics. Fresh frozen samples were collected from 3 animals in each treatment cohort 12 days after tumour engraftment. Tumour samples were snap frozen in RNAlater (Thermo Fisher Scientific) and stored at -80°C prior to RNA extraction. Samples were processed by homogenization using a Precellys24 homogenizer (Bertin Technologies, Montigny, France) and RNA was extracted using an RNeasy mini kit (Qiagen Ltd, Crawley, UK). Genomic DNA was removed from 400 ng of total RNA samples using genomic DNA eliminator column from RNeasy Plus Micro Kit (Qiagen Ltd), polyA RNA was selected using the NEBNext mRNA magnetic Isolation Module (New England Biolabs, Cambridge, UK) following manufacturer directions. From the resulting mRNA, Strand-specific libraries were created using NEBNext Ultra II Directional RNA Library Prep Kit for Illumina (New England Biolabs). Final libraries were quantified using qPCR and clustered at a Molarity of 13.5 pM, sequencing was performed on an Illumina HiSeq 2500 using SE x50 cycles RAPID v2 SBS chemistry. The 18 samples were run at 9 samples per lane to achieve coverage of 30-40 million reads per sample. For the bioinformatics, raw count data was normalised to correct for library size and RNA composition bias. Each therapeutic cohort was compared to the untreated controls, which were used as a base to calculate differential gene expression. Read data was filtered prior to analysis by removing (i) any genes with 0 reads across all samples and (ii) non-coding protein genes. Differential

expression analysis was performed in R using the Bioconductor package DESeq2 (version 1.18.1). Pathway analyses were performed using the WebGestaltR package (version 0.1.1).

Statistical analyses. All statistical analyses, with the exception of RNAseq data, were conducted using Graphpad Prism, version 7.0 (San Diego, USA). Grouped data are presented as means ± SEM. Differences between multiple groups were assessed using one- or two-way ANOVA with posthoc analysis using Bonferroni's correction. Differences between two groups were assessed using a two-tailed unpaired t-test. Survival outcomes were compared using the Kaplan Meier method and the log rank test.

Results

PD-1 blockade has limited monotherapy efficacy in BN175 sarcoma

To determine the potential efficacy of PD-1 blockade in BN175 sarcomas, the basal immune landscape of these tumours was characterised. On immunohistochemistry, BN175 sarcomas contained $CD3^+$ tumour-infiltrating lymphocytes (TILs) and expressed PD-L1, the ligand of PD-1 (Figure 1A-C). Expression of PD-L1 was inversely related to the density of TILs, with the majority of TILs located in the tumour periphery where PD-L1 expression was absent (Figure 1D-F). Flow cytometry was used to further characterise the composition of TILs in BN175 sarcomas, revealing both effector and regulatory T cell populations (Figure 1G). BN175 cells were also found to express PD-L1 at baseline *in vitro*, with no further upregulation noted following treatment with IFNγ suggestive of cell-autonomous induction of PD-L1 (Supplementary figure 1A). As no rat-specific anti-PD-1 antibodies are commercially available, the cross-reactivity of mouse-reactive anti-PD-1 antibody (clone J43) was tested. Recombinant rat PD-1 protein was conjugated to flow cytometry beads and stained with the candidate therapeutic antibody or isotype control. Fluorescence was only noted with the therapeutic antibody, indicating that the J43 mouse-reactive anti-PD-1 antibody cross-reacts with rat PD-1 (Supplementary figure 1B). This antibody was then used to determine therapeutic efficacy of PD-1 blockade *in vivo*. PD-1 blockade exerted limited efficacy as monotherapy, causing a significant delay in tumour growth but only a modest improvement in survival (median 10 vs 13 days, $p = 0.006$) (Figure 1H,I). Dose-escalation yielded no further therapeutic benefit, implying that the characteristics of the TME rather than the dosage of anti-PD-1 antibody limited efficacy in this model (Supplementary figure 1C,D).

Viral ILP augments the efficacy of PD-1 blockade in a palliative ILP model

Having demonstrated that anti-PD-1 monotherapy has limited efficacy, we investigated whether pre-treatment with our established regimen of viral ILP (GLV-1h68, melphalan, TNF□) could increase this effect (*25, 26*). Tumour-bearing Brown Norway rats underwent a treatment protocol that mimicked the clinical use of ILP as palliative treatment (Figure 2A). Combination therapy with viral ILP and PD-1 blockade enhanced therapy compared to either modality alone (Figure 2B). However, recurrent disease rapidly developed within the limb (Figure 2C) and, as such, survival was not improved compared with viral ILP alone (Figure 2D). In some cases, local recurrence occurred whilst PD-1 therapy was ongoing, suggesting that compensatory intra-tumoural immunosuppressive mechanisms may be responsible. Furthermore, tumour immune infiltration by both $CD3^+$ and $CD8^+$ T cells was significantly reduced once the humane endpoint was reached following treatment with viral ILP +/- PD-1 blockade compared with untreated controls, suggesting that treatment resistance may involve enhanced immune evasion (Figure 2E-G). The metastatic potential of BN175 sarcoma has previously been described, with lung metastases developing in animals surviving beyond 30 days post-implantation (*26*). Lung metastases were noted in all animals that survived beyond this point, always in association with locally recurrent disease, indicating the ability of resistant tumours to evade systemic immune surveillance (Figure 2H,I).

Viral ILP with PD-1 blockade secures local and distant disease control in a neoadjuvant model

Although viral ILP and PD-1 blockade improved initial therapy, control of local and distant disease was not achieved in this aggressive model. However, we saw that the enhanced initial response to therapy offered a window of opportunity for further intervention. ILP can be used

clinically as a neoadjuvant pre-operative treatment. We hypothesised that surgical resection of regressing tumours after viral ILP could prevent the evolution of resistant disease and secure durable control of local and distant disease. To investigate this hypothesis, a modified protocol of neoadjuvant viral ILP was developed (Figure 3A). Following ILP, a compartmentectomy was performed to remove the tumour en-bloc within the biceps femoris muscle, with the aim of achieving negative circumferential surgical margins (Figure 3B). At the time of resection, tumour volumes were significantly smaller in rats treated with viral ILP combined with PD-1 blockade (Figure 3C). Whereas local recurrence occurred in two-thirds of animals treated with viral ILP alone, no local relapses were noted in the combination therapy cohort (Figure 3D,E). The combination of viral ILP with PD-1 blockade significantly improved survival compared with viral ILP alone ($p = 0.018$) (Figure 3F). Metastatic disease developed in a third of animals treated with viral ILP alone, with one animal euthanized for symptomatic pulmonary lesions, whereas no evidence of metastatic disease was found in the combination therapy cohort (Figure 3G). As such, all animals in the combination cohort were cured of local and distant disease.

GLV-1h68 and PD-1 blockade are both required for cure

Having demonstrated that viral ILP and PD-1 blockade was able to secure local and systemic disease control, we sought to determine the importance of GLV-1h68 in increasing sensitivity to PD-1 inhibition. In order to do so, tumour-bearing Brown Norway rats underwent the same neoadjuvant ILP protocol as described above, but without the addition of GLV-1h68. At the time of tumour resection, no difference in tumour volume was noted with the addition of PD-1 blockade to standard ILP, although a marked reduction in tumour volume was noted in 2 out of 9 subjects receiving the PD-1 inhibitor (Supplementary figure 3A). Animals receiving standard

ILP and anti-PD-1 antibodies had a lower incidence of local recurrence compared with standard ILP alone (Supplementary figure 3B,C). However, symptomatic metastases developed in 2 of these animals. As a result, the addition of anti-PD-1 antibodies to standard ILP did not improve survival when compared with standard ILP alone (Supplementary figure 3D).

Melphalan and GLV-1h68 induce markers of immunogenic cell death in vitro

We then sought to determine the possible mechanism by which melphalan and GLV-1h68 improve the efficacy of PD-1 blockade. The manner of cell death is known to influence the generation of anti-tumour immune responses. Immunogenic cell death is characterised by the production of several damage associated molecular patterns (DAMPs), with release of ATP, cell surface calreticulin (CRT) and secreted HMGB1 thought to be the most vital to establishing anti-tumour immune responses (*30*).

We have previously shown that melphalan and GLV-1h68 are cytotoxic in both rat and human sarcoma cell lines, with at least an additive effect with combined therapy *in vitro* (*25*). Although treatment with melphalan induced marked secretion of ATP from BN175 cells, only modest secretion was noted in one human sarcoma cell line (Supplementary figure 4A-C). In contrast, GLV-1h68 induced substantial secretion of ATP in all lines tested (Supplementary figure 4D-F). Similarly, melphalan significantly increased cell surface CRT expression in the BN175 and SW872 cell lines but not in HT1080 cells (Supplementary figure 4G-I). However, GLV-1h68 led to increase CRT expression in all cell lines, to consistently higher levels than noted with melphalan (Supplementary figure 4J-L). Significant increases in secreted HMGB1 were seen in all cell lines treated with either melphalan or GLV-1h68, with the highest levels noted after viral infection (Supplementary figure 4M-O).

Viral ILP and PD-1 blockade promotes intra-tumoural immune infiltration

In order to determine the effects of therapy on the TME *in vivo*, tumours and tumour-draining lymph nodes were collected from 3 animals in each cohort at the time of surgery and analysed by flow cytometry (representative gating strategies in Supplementary figure 5). Combination treatment with viral ILP and PD-1 blockade significantly increased the number of tumour-infiltrating $CD3^+$ T cells (Figure 4A). This comprised a significant increase in both $CD8^+$ cytotoxic T cells and $CD4^+$ $Foxp3^-$ effector T cells (Figure 4B,C). No significant change in $CD4^+$ $Foxp3^+$ regulatory T cells was noted (Supplementary figure 6A), although a trend towards an increase was seen with all ILP-based therapies. Viral ILP, with or without PD-1 blockade, also significantly increased the proportion of $CD8^+$ T cells expressing the activation marker Granzyme B compared with untreated controls (Figure 4D). No significant difference in tumour infiltration by $CD3^-$ $CD161^+$ NK cells was noted (Supplementary figure 6B), although again a trend towards an increase was seen in the viral ILP cohorts. Both viral ILP alone and its combination with PD-1 blockade caused an increase in overall immune infiltration of the tumour when compared with other therapies (Supplementary figure 6C). Although no significant differences were noted within individual immune subsets, viral ILP and PD-1 blockade also increased immune infiltration within tumour-draining lymph nodes, harvested from above the level of the tourniquet and, therefore, outside of the perfusion field (Supplementary figure 6D). As such, viral ILP with PD-1 blockade not only resulted in increased immune infiltration of the tumour but also promoted immune infiltration in lymph nodes located outside of the perfusion field, indicative of at least a locoregional and, perhaps, a systemic immune-priming effect.

Viral ILP and PD-1 blockade alters the topography of CD8$^+$ T cell infiltration.

Having found that viral ILP and PD-1 blockade most notably increased infiltration by CD8$^+$ cytotoxic T cells, we sought to determine whether treatment altered the topography of these cells within BN175 sarcomas. Using tumours collected on day 12 following treatment with viral ILP +/- anti-PD-1 antibodies, the density of CD8$^+$ cytotoxic T cells at both the invasive margin and within the tumour parenchyma was quantified. In untreated tumours, although CD8$^+$ cytotoxic T cells were present, the majority were limited to the invasive margin with very few found within the tumour parenchyma equating to an immune-excluded phenotype (*31*). The density of CD8$^+$ cytotoxic T cells at both the invasion margin (Figure 4E, Supplementary figure 7A-F) and within the parenchyma (Figure 4F, Supplementary Figure 7G-L) was significantly increased with all ILP-based treatments, with the most marked increase seen with viral ILP and PD-1 blockade. Indeed, viral ILP and PD-1 blockade completely reversed the topography of CD8$^+$ cytotoxic T cells infiltration, significantly increased infiltration of the tumour parenchyma compared with the invasive margin (Figure 4G-I).

Viral ILP and PD-1 blockade alters intra-tumoural gene expression

Although evidence of increased effector T cell infiltration was noted in all ILP-based therapies, only the combination of viral ILP and PD-1 blockade resulted in long-term disease control at local and distant sites. Cognisant of the potential contribution of other intra-tumoural immune populations and various chemo/cytokines to cure, we sought to further interrogate alterations in the tumour microenvironment using RNAseq, utilising RNA extracted from the same tumour samples analysed by flow cytometry.

Pathway analyses demonstrated evidence of the immune-priming effects of viral ILP. The top 10 up-regulated pathways following viral ILP included antigen processing and presentation (rno04612), Th1 and Th2 cell differentiation (rno04658) and Th17 cell differentiation (rno04569). Furthermore, all of the remaining top up-regulated pathways were immune-based being involved in infectious or autoimmune responses (Supplementary table 1). In contrast, none of these pathways was amongst the top 10 up-regulated following ILP alone.

The relative proportions of intra-tumoural immune cell populations were calculated using CIBERSORT (Figure 4J) (*32*). The most prominent immune subset present at baseline was macrophages, expressing a predominantly M2-like phenotype. Treatment with ILP alone promoted a more immunosuppressive environment, with an expansion in the proportion of regulatory T cells and a reduction in $CD8^+$ T cells. The addition of anti-PD-1 to ILP lead to an expansion of $CD8^+$ T cells without reducing the regulatory T cell population, a potential reason for the lack of benefit noted with this combination therapy. In contrast, viral ILP promoted a more favourable TME, with a dramatic reduction in the proportion of regulatory T cells with an increase in $CD8^+$ T cells when compared with ILP alone. However, the most marked difference between therapies was noted with viral ILP and PD-1 blockade, which in addition to increasing the proportions of effector T cells also led to a substantial reduction in M2-like macrophages and the accumulation of intra-tumoural dendritic cells (DCs). CIBERSORT also allows an estimation of the relative abundance of immune populations (Supplementary figure 8A). Viral ILP and PD-1 blockade led to an almost 3-fold increase in total infiltration when compared with controls, demonstrating increases in absolute terms of both $CD8^+$ T cells and DCs.

Having demonstrated such an increase in DCs with our curative regime, we sought to determine the activation status of these cells. Significant upregulation of a number of genes

known to be associated with an activated state in DCs was noted following viral ILP and PD-1 blockade, in stark contrast to the other cohorts (Supplementary figure 8B) (*33*). This is suggestive that not only did this combination therapy increase the number of intra-tumoural DCs but also augmented their function.

Alterations in the expression of various chemo/cytokines were noted in all therapeutic cohorts (Supplementary figure 8C-F). However, the majority of alterations were seen following treatment with viral ILP and PD-1 blockade. Furthermore, the expression of a number of chemo/cytokines was exclusively altered in this cohort. Within the CCL family, up-regulation of the CCR1 receptor was only noted in this cohort, alongside increased expression of its ligands CCL3 and CCL5. Other exclusive alterations in the CCL family included up-regulation of CCL4 and down-regulation CCL27. Within the CXCL family, the only exclusive alteration with viral ILP and PD-1 blockade was the up-regulation of CXCL2, with increased expression of its receptor CXCR2 also noted. Multiple exclusive alterations in expression were noted in the interleukins with up-regulation of IL-6, IL-15 and IL-17b and down-regulation of IL-24 with concordant alterations in the expression of their relevant receptors (IL-6r, IL15ra, IL17ra/rd, IL20rb).

Further evidence of a favourable modulation of the TME following VV-ILP and PD-1 blockade was noted in the expression of genes recognized be adversely or favourably prognostic across a range of cancers (*34*). VV-ILP and PD-1 blockade led to significant down regulation of all of the top 10 adversely prognostic pan-cancer genes, in contrast to all other therapeutic cohorts (Supplementary figure 8G). In addition, this treatment led to the up regulation of the majority of the top 10 favourably prognostic pan-cancer genes (*Itm2b, Cbx7, Cd2, Satb1, Saraf, Fuca1*) (Supplementary figure 8H).

Discussion

There is a great need for novel therapies that can both prevent the development of and effectively treat metastatic sarcoma. The successes of immunotherapy in non-sarcomatous pathologies have not yet been replicated in sarcoma, which is generally viewed as a non-immunogenic malignancy. Hence there is a great interest in identifying novel therapeutic combinations that may augment anti-tumour immune responses in sarcoma. Here we demonstrate the ability of an oncolytic virus delivered by ILP to dramatically alter the TME in soft-tissue sarcoma. In doing so, viral ILP markedly increased the efficacy of PD-1 inhibition leading to durable cures.

The potential for various viruses to synergise with immune checkpoint inhibitors in non-sarcomatous pathologies has now been demonstrated in both pre-clinical and clinical studies (*35-38*). The optimal route of viral delivery remains the topic of much debate. In all except one of the studies above, virus was delivered by intra-tumoural injection (*35, 36, 38*). Whilst this is an effective strategy in both mice and men with subcutaneous disease, it may be a less practical approach in sarcoma due to the size and depth of these lesions. Systemic delivery would be preferable but is yet to demonstrate clinical benefit in solid tumours (*21, 23*). Locoregional delivery of virus via ILP allows many of the barriers met with systemic administration to be overcome and we have previously shown this route of delivery to be more effective than systemic delivery (*25, 26*).

The combination of viral ILP with PD-1 blockade dramatically altered the TME in BN175 sarcoma. Not only did this treatment increase the number of $CD4^+$ and $CD8^+$ effectors cells within the tumour, but it also increased their expression of activation markers (Figure 4A-D).

Increased infiltration by effector cells was not accompanied by expansion of intra-tumoural regulatory T cells tipping the balance in favour of anti-tumour immune responses. Furthermore, this treatment radically modified the topography of immune infiltration within the tumour. Untreated BN175 sarcoma demonstrated an immune-excluded phenotype, with $CD8^+$ infiltration limited to the invasive margin and sparse infiltration of the tumour parenchyma. Although infiltration at both sites increased following viral ILP and PD-1 blockade, the preferential expansion of parenchymal $CD8^+$ cells led to a complete reversal of the topography of infiltration (Figure 4E-I).

Location rather than presence of TILs is thought to be increasingly important in both response and resistance to immune checkpoint blockade. Whilst the presence of $CD8^+$ TILs at the invasive margin has been found to be predictive of response to PD-1 blockade in patients with melanoma, responders were characterised by expansion of these cells within the tumour (*18*). Again in melanoma, patients who relapsed after PD-1 therapy were found to have fewer $CD8^+$ TILs that were limited to the margin of the tumour when compared with their original lesion (*39*). Similar features were seen with relapse following viral ILP and PD-1 blockade in our model (Figure 2E-G). Our data attach a similar importance to the location of TILs in this model of sarcoma, demonstrating that oncolytic viruses can induce favourable topographical changes in the sarcoma TME.

In trying to predict how responses to immune checkpoint blockade may be maximised, and how oncolytic viruses may facilitate such augmentation, much of the focus has been on T cells, in particular cytotoxic $CD8^+$ T cells. Although significant alterations in both $CD8^+$ T cell

infiltration and distribution within the tumour were noted in our curative regimen, similar changes, albeit to a lesser extent, were noted in other therapeutic cohorts that were compromised by both local and distant relapse. This suggests that the engagement of other immune cell populations is critical to engendering anti-tumour immunity. Our data suggest that the critical population in this process are DCs, with a marked expansion of this population only noted with our curative regimen. By processing and presenting antigen, DCs play a vital role in activating the adaptive immune system and so it follows that the engagement of this cell population is critical in generating systemic anti-tumour immunity following a local therapy (*40*). DCs are known to express both PD-L1 and PD-L2 and blockade of the PD-1 axis has been shown to promote the ability of these cells to stimulate effector T cell functions (*41*). Hence, whilst viral ILP may promote a more inflamed TME characterised by increased infiltration by T cell effectors, its efficacy may be limited by tumour mechanisms of immunosuppression. The additional blockade of PD-1 may then disinhibit DCs to stimulate a more effective, durable anti-tumour immune response. Given the complexity of the curative regimen utilized in this model, it is possible that the other therapeutics may also be implicated in this process, most notably TNFα, which has been shown to enhance DC maturation (*42*). However, given that no substantial alteration in DCs was noted following standard ILP with or without subsequent PD-1 blockade, it does not appear that TNFα is critical to the expansion of this cell population in this model.

Alterations in the chemokine profile of BN175 sarcoma support the importance of DCs to cure. CCL4 was exclusively up-regulated in the curative regimen and has been previously shown to play a critical role in the recruitment of DCs in both clinical and pre-clinical models of melanoma (*43*). A lack of intra-tumoural DCs was associated with limited response to

checkpoint blockade, a phenotype that was reversed if these cells were then delivered by intra-tumoural injection. CCL3 and CCL5 have also been shown to play a role in both T cell and DC recruitment in models of melanoma and colorectal cancer (*44*, *45*). Whilst these chemokines were also upregulated in other therapeutic cohorts in our model, their receptor CCR1 was only upregulated in the curative regimen, suggesting greater activity of this axis. Furthermore, only viral ILP and PD-1 blockade led to increased expression of IL-6, which has been shown to be critical for the effective induction of T_H17 cells by DCs (*46*).

Our data also highlight the importance of combining immunotherapy with effective local therapies to maximise its curative potential. The evolution of resistant disease is well recognised in patients receiving immune checkpoint inhibitors for melanoma, although the responsible mechanisms are complex and still under investigation (*39*, *47*). Such lesions are typically unresponsive to further therapy, portending poor outcomes. In our palliative model, in which the tumour remains in situ, an initial improvement in therapy was seen when combining viral ILP with PD-1 blockade but resistant disease rapidly developed leading to both local and distant treatment failure (Figure 2). In contrast, effective local treatment with early surgical resection and adjuvant radiotherapy of regressing tumours led to durable cures (Figure 3). The combination of surgery, GLV-1h68 and PD-1 blockade were crucial to cure, as the removal of any part of this protocol was associated with relapse. Similar results have been demonstrated with the neoadjuvant administration of Maraba virus prior to surgery in a model of triple negative breast cancer (*48*). It may be that such neoadjuvant strategies allow the generation of an effective anti-tumour immune response, which eliminated micrometastatic disease, whilst simultaneously preventing the evolution of resistance by effectively treating the primary tumour.

The authors recognize certain limitations of this study. As the *in vivo* experiments were conducted in a single tumour model, the results on the TME at baseline and it's transformation following therapy, should be interpreted with caution in the context of the diverse histological subtypes seen in human soft-tissue sarcoma. We have previously attempted to classify the BN175 tumour with standard immunohistochemical stains (S100, desmin, smooth muscle actin, caldesmon and Factor VIII). The only positive marker was Factor VIII, typically associated with angiosarcoma. However, morphologically, this tumour is not typical of a liposarcoma or angiosarcoma and was felt to be more in keeping with an undifferentiated pleomorphic sarcoma. Several studies have sought to delineate the TME in soft-tissue sarcoma, although they are limited by both diversity in the histological subtypes included and the methods employed. In translational analyses of baseline samples from patients enrolled in a phase II study combining pembrolizumab with cyclophosphamide, CD8 T cell infiltration was low, as seen in the BN175 tumours (*13*). However, PD-L1 expression was also low, positive in only 6 of 50 patients, and co-localization rather than exclusion of CD8 T cells was noted. In contrast, whilst studies of historical pathological samples have demonstrated similar results in terms of CD8/PD-L1 co-localization, markedly higher levels of both PD-L1 expression and T cell infiltration were found (*49-51*). As the vaccinia virus has no known entry receptor, one would hypothesize that viral infection would not limit the applicability of this approach to diverse histological subtypes. However, given the variability in the biological behaviours noted between these subtypes, the ability of infection to lead to a transformation of the TME and subsequent sensitivity to PD-1 blockade should not be assumed and requires confirmation in the clinical setting.

The combination of viral and PD-1 blockade prior to surgery has the potential for direct clinical translation. ILP is often used in the neoadjuvant setting prior to surgery for soft-tissue sarcomas (*28*). A function-preserving resection is typically performed between 6-8 weeks later, followed by adjuvant radiotherapy if viable tumour is found within the specimen. Although typically reserved for patients with locally advanced tumours, our data provide a rationale for extending the use of a modified neoadjuvant protocol to those patients at greatest risk of systemic relapse. Such patients are readily identifiable at diagnosis by such factors as tumour size, grade and histological subtype (*52*). As an alternative to standard practice, these high-risk patients could undergo a viral ILP followed by administration of anti-PD-1 antibodies for the 6-8 weeks prior to surgery, which could continue thereafter. A Phase I study to determine the tolerability and safety of combining OV and ILP, and to identify predictive biomarkers of response, is currently recruiting (NCT0355502). While it is recognised that trials combining such novel treatments are typically reserved for patients with established metastatic disease, our data add to an increasing body of evidence in various pathologies supporting the use of combination immunotherapies in early stage disease.

Acknowledgments: RNAseq and bioinformatics were performed by Kerry Fenwick, Alistair Rust and Nik Matthews of the Tumour Profiling Unit (TPU) at The Institute of Cancer Research (ICR). The authors are indebted to Professor A Eggermont for the donation of the BN175 cell line. **Funding**: HGS received academic grants from The Royal College of Surgeons of England (160729), Sarcoma UK (SUK203.2016 / SUK203.2017), The Meirion Thomas Cancer Research Fund and The McAlpine Foundation. VR and JNKC were funded by Oracle Cancer Trust/The Mark Donegan Foundation. JTP and AAK were funded by the Wellcome Trust (WT098937MF; 200175/Z/15). KJH acknowledges funding from the Rosetrees Trust (A1292). AM, KT, KJH and AJH acknowledge support from The Royal Marsden/The Institute of Cancer Research, National Institute for Health Research Biomedical Research Centre (NIHR BRC). **Author contributions**: HGS, KJH and AJH contributed to the study design and conceptualization. HGS and MM conducted the *in vivo* studies. HGS, DM, VR, JNKC and JTP designed and performed the *in vitro* studies. HGS, RP, and KB designed and performed the flow cytometry studies. HGS, MM and KT performed the immunohistochemistry studies. HGS, KJH and AJH wrote the manuscript. MTD, AAK, and AAM performed critical review of the data and manuscript. **Competing interests**: The authors declare they have no competing interests. **Data and materials availability**: Materials can be obtained from The Institute of Cancer Research (ICR) by a material transfer agreement.

References:

1. C. A. Stiller, A. Trama, D. Serraino, S. Rossi, C. Navarro, M. D. Chirlaque, P. G. Casali, R. W. Group, Descriptive epidemiology of sarcomas in Europe: report from the RARECARE project. *Eur J Cancer* **49**, 684-695 (2013).
2. M. F. Brennan, C. R. Antonescu, N. Moraco, S. Singer, Lessons learned from the study of 10,000 patients with soft tissue sarcoma. *Ann Surg* **260**, 416-421; discussion 421-412 (2014).
3. E. S. E. S. N. W. Group, Soft tissue and visceral sarcomas: ESMO Clinical Practice Guidelines for diagnosis, treatment and follow-up. *Annals of oncology : official journal of the European Society for Medical Oncology / ESMO* **25 Suppl 3**, iii102-112 (2014).
4. H. G. Smith, N. Memos, J. M. Thomas, M. J. Smith, D. C. Strauss, A. J. Hayes, Patterns of disease relapse in primary extremity soft-tissue sarcoma. *Br J Surg* **103**, 1487-1496 (2016).
5. A. Gronchi, S. Lo Vullo, C. Colombo, P. Collini, S. Stacchiotti, L. Mariani, M. Fiore, P. G. Casali, Extremity soft tissue sarcoma in a series of patients treated at a single institution: local control directly impacts survival. *Ann Surg* **251**, 506-511 (2010).
6. A. Gronchi, S. Ferrari, V. Quagliuolo, J. M. Broto, A. L. Pousa, G. Grignani, U. Basso, J. Y. Blay, O. Tendero, R. D. Beveridge, V. Ferraresi, I. Lugowska, D. F. Merlo, V. Fontana, E. Marchesi, D. M. Donati, E. Palassini, E. Palmerini, R. De Sanctis, C. Morosi, S. Stacchiotti, S. Bague, J. M. Coindre, A. P. Dei Tos, P. Picci, P. Bruzzi, P. G. Casali, Histotype-tailored neoadjuvant chemotherapy versus standard chemotherapy in patients with high-risk soft-tissue sarcomas (ISG-STS 1001): an international, open-label, randomised, controlled, phase 3, multicentre trial. *The Lancet. Oncology* **18**, 812-822 (2017).
7. P. J. Woll, P. Reichardt, A. Le Cesne, S. Bonvalot, A. Azzarelli, H. J. Hoekstra, M. Leahy, F. Van Coevorden, J. Verweij, P. C. Hogendoorn, M. Ouali, S. Marreaud, V. H. Bramwell, P. Hohenberger, E. S. Tissue, G. Bone Sarcoma, N. C. T. G. S. D. S. C. the, Adjuvant chemotherapy with doxorubicin, ifosfamide, and lenograstim for resected soft-tissue sarcoma (EORTC 62931): a multicentre randomised controlled trial. *The Lancet. Oncology* **13**, 1045-1054 (2012).
8. I. Judson, J. Verweij, H. Gelderblom, J. T. Hartmann, P. Schoffski, J. Y. Blay, J. M. Kerst, J. Sufliarsky, J. Whelan, P. Hohenberger, A. Krarup-Hansen, T. Alcindor, S. Marreaud, S. Litiere, C. Hermans, C. Fisher, P. C. Hogendoorn, A. P. dei Tos, W. T. van der Graaf, O. European, T. Treatment of Cancer Soft, G. Bone Sarcoma, Doxorubicin alone versus intensified doxorubicin plus ifosfamide for first-line treatment of advanced or metastatic soft-tissue sarcoma: a randomised controlled phase 3 trial. *The Lancet. Oncology* **15**, 415-423 (2014).
9. M. Maio, J. J. Grob, S. Aamdal, I. Bondarenko, C. Robert, L. Thomas, C. Garbe, V. Chiarion-Sileni, A. Testori, T. T. Chen, M. Tschaika, J. D. Wolchok, Five-year survival rates for treatment-naive patients with advanced melanoma who received ipilimumab plus dacarbazine in a phase III trial. *J Clin Oncol* **33**, 1191-1196 (2015).
10. D. Schadendorf, F. S. Hodi, C. Robert, J. S. Weber, K. Margolin, O. Hamid, D. Patt, T. T. Chen, D. M. Berman, J. D. Wolchok, Pooled Analysis of Long-Term Survival Data From Phase II and Phase III Trials of Ipilimumab in Unresectable or Metastatic Melanoma. *J Clin Oncol* **33**, 1889-1894 (2015).
11. S. L. Topalian, M. Sznol, D. F. McDermott, H. M. Kluger, R. D. Carvajal, W. H. Sharfman, J. R. Brahmer, D. P. Lawrence, M. B. Atkins, J. D. Powderly, P. D. Leming, E. J. Lipson, I. Puzanov, D. C. Smith, J. M. Taube, J. M. Wigginton, G. D. Kollia, A. Gupta, D. M. Pardoll, J. A. Sosman, F. S. Hodi, Survival, durable tumor remission, and long-term safety in patients with advanced melanoma receiving nivolumab. *J Clin Oncol* **32**, 1020-1030 (2014).
12. H. A. Tawbi, M. Burgess, V. Bolejack, B. A. Van Tine, S. M. Schuetze, J. Hu, S. D'Angelo, S. Attia, R. F. Riedel, D. A. Priebat, S. Movva, L. E. Davis, S. H. Okuno, D. R. Reed, J. Crowley, L. H. Butterfield, R. Salazar, J. Rodriguez-Canales, A. J. Lazar, Wistuba, II, L. H. Baker, R. G. Maki, D. Reinke, S. Patel, Pembrolizumab in advanced soft-tissue sarcoma and bone sarcoma (SARC028): a multicentre, two-cohort, single-arm, open-label, phase 2 trial. *The Lancet. Oncology* **18**, 1493-1501 (2017).
13. M. Toulmonde, N. Penel, J. Adam, C. Chevreau, J. Y. Blay, A. Le Cesne, E. Bompas, S. Piperno-Neumann, S. Cousin, T. Grellety, T. Ryckewaert, A. Bessede, F. Ghiringhelli, M. Pulido, A. Italiano, Use of PD-1 Targeting, Macrophage Infiltration, and IDO Pathway Activation in Sarcomas: A Phase 2 Clinical Trial. *JAMA Oncol* **4**, 93-97 (2018).
14. M. Ayers, J. Lunceford, M. Nebozhyn, E. Murphy, A. Loboda, D. R. Kaufman, A. Albright, J. D. Cheng, S. P. Kang, V. Shankaran, S. A. Piha-Paul, J. Yearley, T. Y. Seiwert, A. Ribas, T. K. McClanahan, IFN-

gamma-related mRNA profile predicts clinical response to PD-1 blockade. *J Clin Invest* **127**, 2930-2940 (2017).

15. A. I. Daud, J. D. Wolchok, C. Robert, W. J. Hwu, J. S. Weber, A. Ribas, F. S. Hodi, A. M. Joshua, R. Kefford, P. Hersey, R. Joseph, T. C. Gangadhar, R. Dronca, A. Patnaik, H. Zarour, C. Roach, G. Toland, J. K. Lunceford, X. N. Li, K. Emancipator, M. Dolled-Filhart, S. P. Kang, S. Ebbinghaus, O. Hamid, Programmed Death-Ligand 1 Expression and Response to the Anti-Programmed Death 1 Antibody Pembrolizumab in Melanoma. *J Clin Oncol* **34**, 4102-4109 (2016).
16. A. M. Goodman, S. Kato, L. Bazhenova, S. P. Patel, G. M. Frampton, V. Miller, P. J. Stephens, G. A. Daniels, R. Kurzrock, Tumor Mutational Burden as an Independent Predictor of Response to Immunotherapy in Diverse Cancers. *Mol Cancer Ther* **16**, 2598-2608 (2017).
17. T. Y. Seiwert, B. Burtness, R. Mehra, J. Weiss, R. Berger, J. P. Eder, K. Heath, T. McClanahan, J. Lunceford, C. Gause, J. D. Cheng, L. Q. Chow, Safety and clinical activity of pembrolizumab for treatment of recurrent or metastatic squamous cell carcinoma of the head and neck (KEYNOTE-012): an open-label, multicentre, phase 1b trial. *The Lancet. Oncology* **17**, 956-965 (2016).
18. P. C. Tumeh, C. L. Harview, J. H. Yearley, I. P. Shintaku, E. J. Taylor, L. Robert, B. Chmielowski, M. Spasic, G. Henry, V. Ciobanu, A. N. West, M. Carmona, C. Kivork, E. Seja, G. Cherry, A. J. Gutierrez, T. R. Grogan, C. Mateus, G. Tomasic, J. A. Glaspy, R. O. Emerson, H. Robins, R. H. Pierce, D. A. Elashoff, C. Robert, A. Ribas, PD-1 blockade induces responses by inhibiting adaptive immune resistance. *Nature* **515**, 568-571 (2014).
19. S. Turnbull, E. J. West, K. J. Scott, E. Appleton, A. Melcher, C. Ralph, Evidence for Oncolytic Virotherapy: Where Have We Got to and Where Are We Going? *Viruses* **7**, 6291-6312 (2015).
20. R. H. Andtbacka, H. L. Kaufman, F. Collichio, T. Amatruda, N. Senzer, J. Chesney, K. A. Delman, L. E. Spitler, I. Puzanov, S. S. Agarwala, M. Milhem, L. Cranmer, B. Curti, K. Lewis, M. Ross, T. Guthrie, G. P. Linette, G. A. Daniels, K. Harrington, M. R. Middleton, W. H. Miller, Jr., J. S. Zager, Y. Ye, B. Yao, A. Li, S. Doleman, A. VanderWalde, J. Gansert, R. S. Coffin, Talimogene Laherparepvec Improves Durable Response Rate in Patients With Advanced Melanoma. *Journal of clinical oncology : official journal of the American Society of Clinical Oncology*, (2015).
21. R. A. Adair, V. Roulstone, K. J. Scott, R. Morgan, G. J. Nuovo, M. Fuller, D. Beirne, E. J. West, V. A. Jennings, A. Rose, J. Kyula, S. Fraser, R. Dave, D. A. Anthoney, A. Merrick, R. Prestwich, A. Aldouri, O. Donnelly, H. Pandha, M. Coffey, P. Selby, R. Vile, G. Toogood, K. Harrington, A. A. Melcher, Cell carriage, delivery, and selective replication of an oncolytic virus in tumor in patients. *Sci Transl Med* **4**, 138ra177 (2012).
22. A. Dispenzieri, C. Tong, B. LaPlant, M. Q. Lacy, K. Laumann, D. Dingli, Y. Zhou, M. J. Federspiel, M. A. Gertz, S. Hayman, F. Buadi, M. O'Connor, V. J. Lowe, K. W. Peng, S. J. Russell, Phase I trial of systemic administration of Edmonston strain of measles virus genetically engineered to express the sodium iodide symporter in patients with recurrent or refractory multiple myeloma. *Leukemia* **31**, 2791-2798 (2017).
23. S. H. Park, C. J. Breitbach, J. Lee, J. O. Park, H. Y. Lim, W. K. Kang, A. Moon, J. H. Mun, E. M. Sommermann, L. Maruri Avidal, R. Patt, A. Pelusio, J. Burke, T. H. Hwang, D. Kirn, Y. S. Park, Phase 1b Trial of Biweekly Intravenous Pexa-Vec (JX-594), an Oncolytic and Immunotherapeutic Vaccinia Virus in Colorectal Cancer. *Mol Ther* **23**, 1532-1540 (2015).
24. A. Samson, K. J. Scott, D. Taggart, E. J. West, E. Wilson, G. J. Nuovo, S. Thomson, R. Corns, R. K. Mathew, M. J. Fuller, T. J. Kottke, J. M. Thompson, E. J. Ilett, J. V. Cockle, P. van Hille, G. Sivakumar, E. S. Polson, S. J. Turnbull, E. S. Appleton, G. Migneco, A. S. Rose, M. C. Coffey, D. A. Beirne, F. J. Collinson, C. Ralph, D. Alan Anthoney, C. J. Twelves, A. J. Furness, S. A. Quezada, H. Wurdak, F. Errington-Mais, H. Pandha, K. J. Harrington, P. J. Selby, R. G. Vile, S. D. Griffin, L. F. Stead, S. C. Short, A. A. Melcher, Intravenous delivery of oncolytic reovirus to brain tumor patients immunologically primes for subsequent checkpoint blockade. *Sci Transl Med* **10**, (2018).
25. T. D. Pencavel, M. J. Wilkinson, D. C. Mansfield, A. A. Khan, R. Seth, E. M. Karapanagiotou, V. Roulstone, R. J. Aguilar, N. G. Chen, A. A. Szalay, A. J. Hayes, K. J. Harrington, Isolated limb perfusion with melphalan, tumour necrosis factor-alpha and oncolytic vaccinia virus improves tumour targeting and prolongs survival in a rat model of advanced extremity sarcoma. *Int J Cancer* **136**, 965-976 (2015).
26. M. J. Wilkinson, H. G. Smith, T. D. Pencavel, D. C. Mansfield, J. Kyula-Currie, A. A. Khan, G. McEntee, V. Roulstone, A. J. Hayes, K. J. Harrington, Isolated limb perfusion with biochemotherapy and oncolytic virotherapy combines with radiotherapy and surgery to overcome treatment resistance in an animal model of extremity soft tissue sarcoma. *Int J Cancer* **139**, 1414-1422 (2016).

27. A. M. Eggermont, J. H. de Wilt, T. L. ten Hagen, Current uses of isolated limb perfusion in the clinic and a model system for new strategies. *The Lancet. Oncology* **4**, 429-437 (2003).
28. A. M. Eggermont, H. Schraffordt Koops, J. M. Klausner, B. B. Kroon, P. M. Schlag, D. Lienard, A. N. van Geel, H. J. Hoekstra, I. Meller, O. E. Nieweg, C. Kettelhack, G. Ben-Ari, J. C. Pector, F. J. Lejeune, Isolated limb perfusion with tumor necrosis factor and melphalan for limb salvage in 186 patients with locally advanced soft tissue extremity sarcomas. The cumulative multicenter European experience. *Ann Surg* **224**, 756-764; discussion 764-755 (1996).
29. H. G. Smith, J. Cartwright, M. J. Wilkinson, D. C. Strauss, J. M. Thomas, A. J. Hayes, Isolated Limb Perfusion with Melphalan and Tumour Necrosis Factor alpha for In-Transit Melanoma and Soft Tissue Sarcoma. *Ann Surg Oncol* **22 Suppl 3**, S356-361 (2015).
30. O. Kepp, L. Senovilla, I. Vitale, E. Vacchelli, S. Adjemian, P. Agostinis, L. Apetoh, F. Aranda, V. Barnaba, N. Bloy, L. Bracci, K. Breckpot, D. Brough, A. Buque, M. G. Castro, M. Cirone, M. I. Colombo, I. Cremer, S. Demaria, L. Dini, A. G. Eliopoulos, A. Faggioni, S. C. Formenti, J. Fucikova, L. Gabriele, U. S. Gaipl, J. Galon, A. Garg, F. Ghiringhelli, N. A. Giese, Z. S. Guo, A. Hemminki, M. Herrmann, J. W. Hodge, S. Holdenrieder, J. Honeychurch, H. M. Hu, X. Huang, T. M. Illidge, K. Kono, M. Korbelik, D. V. Krysko, S. Loi, P. R. Lowenstein, E. Lugli, Y. Ma, F. Madeo, A. A. Manfredi, I. Martins, D. Mavilio, L. Menger, N. Merendino, M. Michaud, G. Mignot, K. L. Mossman, G. Multhoff, R. Oehler, F. Palombo, T. Panaretakis, J. Pol, E. Proietti, J. E. Ricci, C. Riganti, P. Rovere-Querini, A. Rubartelli, A. Sistigu, M. J. Smyth, J. Sonnemann, R. Spisek, J. Stagg, A. Q. Sukkurwala, E. Tartour, A. Thorburn, S. H. Thorne, P. Vandenabeele, F. Velotti, S. T. Workenhe, H. Yang, W. X. Zong, L. Zitvogel, G. Kroemer, L. Galluzzi, Consensus guidelines for the detection of immunogenic cell death. *Oncoimmunology* **3**, e955691 (2014).
31. D. S. Chen, I. Mellman, Elements of cancer immunity and the cancer-immune set point. *Nature* **541**, 321-330 (2017).
32. A. M. Newman, C. L. Liu, M. R. Green, A. J. Gentles, W. Feng, Y. Xu, C. D. Hoang, M. Diehn, A. A. Alizadeh, Robust enumeration of cell subsets from tissue expression profiles. *Nat Methods* **12**, 453-457 (2015).
33. A. Torri, O. Beretta, A. Ranghetti, F. Granucci, P. Ricciardi-Castagnoli, M. Foti, Gene expression profiles identify inflammatory signatures in dendritic cells. *PLoS One* **5**, e9404 (2010).
34. A. J. Gentles, A. M. Newman, C. L. Liu, S. V. Bratman, W. Feng, D. Kim, V. S. Nair, Y. Xu, A. Khuong, C. D. Hoang, M. Diehn, R. B. West, S. K. Plevritis, A. A. Alizadeh, The prognostic landscape of genes and infiltrating immune cells across human cancers. *Nat Med* **21**, 938-945 (2015).
35. K. Rajani, C. Parrish, T. Kottke, J. Thompson, S. Zaidi, L. Ilett, K. G. Shim, R. M. Diaz, H. Pandha, K. Harrington, M. Coffey, A. Melcher, R. Vile, Combination Therapy With Reovirus and Anti-PD-1 Blockade Controls Tumor Growth Through Innate and Adaptive Immune Responses. *Mol Ther* **24**, 166-174 (2016).
36. A. Ribas, R. Dummer, I. Puzanov, A. VanderWalde, R. H. I. Andtbacka, O. Michielin, A. J. Olszanski, J. Malvehy, J. Cebon, E. Fernandez, J. M. Kirkwood, T. F. Gajewski, L. Chen, K. S. Gorski, A. A. Anderson, S. J. Diede, M. E. Lassman, J. Gansert, F. S. Hodi, G. V. Long, Oncolytic Virotherapy Promotes Intratumoral T Cell Infiltration and Improves Anti-PD-1 Immunotherapy. *Cell* **170**, 1109-1119 e1110 (2017).
37. J. J. Rojas, P. Sampath, W. Hou, S. H. Thorne, Defining Effective Combinations of Immune Checkpoint Blockade and Oncolytic Virotherapy. *Clin Cancer Res* **21**, 5543-5551 (2015).
38. D. Zamarin, R. B. Holmgaard, S. K. Subudhi, J. S. Park, M. Mansour, P. Palese, T. Merghoub, J. D. Wolchok, J. P. Allison, Localized oncolytic virotherapy overcomes systemic tumor resistance to immune checkpoint blockade immunotherapy. *Sci Transl Med* **6**, 226ra232 (2014).
39. J. M. Zaretsky, A. Garcia-Diaz, D. S. Shin, H. Escuin-Ordinas, W. Hugo, S. Hu-Lieskovan, D. Y. Torrejon, G. Abril-Rodriguez, S. Sandoval, L. Barthly, J. Saco, B. Homet Moreno, R. Mezzadra, B. Chmielowski, K. Ruchalski, I. P. Shintaku, P. J. Sanchez, C. Puig-Saus, G. Cherry, E. Seja, X. Kong, J. Pang, B. Berent-Maoz, B. Comin-Anduix, T. G. Graeber, P. C. Tumeh, T. N. Schumacher, R. S. Lo, A. Ribas, Mutations Associated with Acquired Resistance to PD-1 Blockade in Melanoma. *N Engl J Med* **375**, 819-829 (2016).
40. I. Mellman, R. M. Steinman, Dendritic cells: specialized and regulated antigen processing machines. *Cell* **106**, 255-258 (2001).
41. J. A. Brown, D. M. Dorfman, F. R. Ma, E. L. Sullivan, O. Munoz, C. R. Wood, E. A. Greenfield, G. J. Freeman, Blockade of programmed death-1 ligands on dendritic cells enhances T cell activation and cytokine production. *J Immunol* **170**, 1257-1266 (2003).
42. C. Brunner, J. Seiderer, A. Schlamp, M. Bidlingmaier, A. Eigler, W. Haimerl, H. A. Lehr, A. M. Krieg, G. Hartmann, S. Endres, Enhanced dendritic cell maturation by TNF-alpha or cytidine-phosphate-guanosine

DNA drives T cell activation in vitro and therapeutic anti-tumor immune responses in vivo. *J Immunol* **165**, 6278-6286 (2000).

43. S. Spranger, R. Bao, T. F. Gajewski, Melanoma-intrinsic beta-catenin signalling prevents anti-tumour immunity. *Nature* **523**, 231-235 (2015).
44. F. Allen, I. D. Bobanga, P. Rauhe, D. Barkauskas, N. Teich, C. Tong, J. Myers, A. Y. Huang, CCL3 augments tumor rejection and enhances CD8(+) T cell infiltration through NK and CD103(+) dendritic cell recruitment via IFNgamma. *Oncoimmunology* **7**, e1393598 (2018).
45. H. Harlin, Y. Meng, A. C. Peterson, Y. Zha, M. Tretiakova, C. Slingluff, M. McKee, T. F. Gajewski, Chemokine expression in melanoma metastases associated with CD8+ T-cell recruitment. *Cancer Res* **69**, 3077-3085 (2009).
46. S. Heink, N. Yogev, C. Garbers, M. Herwerth, L. Aly, C. Gasperi, V. Husterer, A. L. Croxford, K. Moller-Hackbarth, H. S. Bartsch, K. Sotlar, S. Krebs, T. Regen, H. Blum, B. Hemmer, T. Misgeld, T. F. Wunderlich, J. Hidalgo, M. Oukka, S. Rose-John, M. Schmidt-Supprian, A. Waisman, T. Korn, Trans-presentation of IL-6 by dendritic cells is required for the priming of pathogenic TH17 cells. *Nat Immunol* **18**, 74-85 (2017).
47. S. J. Patel, N. E. Sanjana, R. J. Kishton, A. Eidizadeh, S. K. Vodnala, M. Cam, J. J. Gartner, L. Jia, S. M. Steinberg, T. N. Yamamoto, A. S. Merchant, G. U. Mehta, A. Chichura, O. Shalem, E. Tran, R. Eil, M. Sukumar, E. P. Guijarro, C. P. Day, P. Robbins, S. Feldman, G. Merlino, F. Zhang, N. P. Restifo, Identification of essential genes for cancer immunotherapy. *Nature* **548**, 537-542 (2017).
48. M. C. Bourgeois-Daigneault, D. G. Roy, A. S. Aitken, N. El Sayes, N. T. Martin, O. Varette, T. Falls, L. E. St-Germain, A. Pelin, B. D. Lichty, D. F. Stojdl, G. Ungerechts, J. S. Diallo, J. C. Bell, Neoadjuvant oncolytic virotherapy before surgery sensitizes triple-negative breast cancer to immune checkpoint therapy. *Sci Transl Med* **10**, (2018).
49. S. P. D'Angelo, A. N. Shoushtari, N. P. Agaram, D. Kuk, L. X. Qin, R. D. Carvajal, M. A. Dickson, M. Gounder, M. L. Keohan, G. K. Schwartz, W. D. Tap, Prevalence of tumor-infiltrating lymphocytes and PD-L1 expression in the soft tissue sarcoma microenvironment. *Hum Pathol* **46**, 357-365 (2015).
50. M. Boxberg, K. Steiger, U. Lenze, H. Rechl, R. von Eisenhart-Rothe, K. Wortler, W. Weichert, R. Langer, K. Specht, PD-L1 and PD-1 and characterization of tumor-infiltrating lymphocytes in high grade sarcomas of soft tissue - prognostic implications and rationale for immunotherapy. *Oncoimmunology* **7**, e1389366 (2018).
51. T. S. Nowicki, R. Akiyama, R. R. Huang, I. P. Shintaku, X. Wang, P. C. Tumeh, A. Singh, B. Chmielowski, C. Denny, N. Federman, A. Ribas, Infiltration of CD8 T Cells and Expression of PD-1 and PD-L1 in Synovial Sarcoma. *Cancer Immunol Res* **5**, 118-126 (2017).
52. D. Callegaro, R. Miceli, S. Bonvalot, P. Ferguson, D. C. Strauss, A. Levy, A. Griffin, A. J. Hayes, S. Stacchiotti, C. L. Pechoux, M. J. Smith, M. Fiore, A. P. Dei Tos, H. G. Smith, L. Mariani, J. S. Wunder, R. E. Pollock, P. G. Casali, A. Gronchi, Development and external validation of two nomograms to predict overall survival and occurrence of distant metastases in adults after surgical resection of localised soft-tissue sarcomas of the extremities: a retrospective analysis. *The Lancet. Oncology* **17**, 671-680 (2016).
53. Q. Zhang, Y. A. Yu, E. Wang, N. Chen, R. L. Danner, P. J. Munson, F. M. Marincola, A. A. Szalay, Eradication of solid human breast tumors in nude mice with an intravenously injected light-emitting oncolytic vaccinia virus. *Cancer Res* **67**, 10038-10046 (2007).
54. L. Kamentsky, T. R. Jones, A. Fraser, M. A. Bray, D. J. Logan, K. L. Madden, V. Ljosa, C. Rueden, K. W. Eliceiri, A. E. Carpenter, Improved structure, function and compatibility for CellProfiler: modular high-throughput image analysis software. *Bioinformatics* **27**, 1179-1180 (2011).

Figures:

Figure 1. Anti-PD-1 monotherapy has limited efficacy in BN175 sarcoma. (A-F) Immunohistochemistry analysis of contiguous sections of untreated tumours (isotype controls **A,D**). BN175 sarcomas contain $CD3^+$ lymphocytes (**B,E**) and express PD-L1 (**C,F**). The dotted red lines in E/F demonstrate areas of high PD-L1 expression corresponding to areas of exclusion of $CD3^+$ lymphocytes. (**G**) Flow cytometry gating strategy to further characterise $CD3^+$ subsets. BN175 sarcomas contain CD4 effector ($CD3^+CD4^+Foxp3^-$) and regulatory populations ($CD3^+CD4^+Foxp3^+$) as well as cytotoxic CD8 T cells ($CD3^+CD8^+$). (H) (**J,K**) Anti-PD-1 monotherapy in BN175 sarcoma. The J43 anti-PD-1 antibody was administered by intraperitoneal injection and compared with an isotype control. Treatment slightly delayed tumour growth (**J**) and modestly improved survival (median survival 10 vs 13 days, $p = 0.006$) ($n = 6$ animals per group) (**K**). ** $P \leq 0.01$; *** $P \leq 0.001$.

Figure 2. Augmented efficacy of PD-1 blockade following viral ILP is limited by the evolution of resistance. (**A**) Operative protocol mimicking palliative ILP in clinical practice, with the addition of anti-PD-1 antibodies. (**B**) Tumour growth curves demonstrating that prior treatment with viral ILP significantly improves response to PD-1 blockade ($n = 6$ animals per group). (**C**) Individual growth curves of animals treated with viral ILP and PD-1 blockade showing the rapid evolution of resistant disease. (**D**) Due to the evolution of resistance, no survival benefit was noted with the addition of PD-1 blockade to viral ILP (median survival 20 versus 31 days, $p = 0.476$). (**E-G**) Immunohistochemistry analysis of tumours at the humane endpoint demonstrated reduced $CD8^+$ immune cell infiltration following treatment with viral ILP +/- PD-1 blockade (**F**) when compared with treatment with an isotype control alone (**E**). (**H-I**) Representative images of pulmonary metastases (black arrows) in animals surviving greater than 30 days following treatment with viral ILP alone (**H**) and combined with PD-1 blockade (**I**). * $P \leq 0.05$; ** $P \leq 0.01$; *** $P \leq 0.001$.

Figure 3. Neoadjuvant viral ILP and PD-1 blockade prior to surgery and radiation secures durable cure. (**A**) Operative protocol mimicking neoadjuvant ILP in clinical practice, with the addition of anti-PD-1 antibodies. (**B**) Surgical resection of the tumour en-bloc within the biceps femoris muscle. (**C**) Tumour volumes at the time of surgery demonstrating increased therapy with the addition of anti-PD-1 antibodies ($n = 9$ animals per group). (**D,E**) Individual growth curves following viral ILP alone (**D**) or in combination with anti-PD-1 antibodies (**E**) prior to surgery (M denotes early termination due to symptomatic metastases) ($n = 6$ animals per group). Viral ILP and PD-1 blockade prevents local and distant relapse prolonging survival when compared with viral ILP alone (**F**) ($p = 0.018$). (**G**) Representative images of pulmonary metastases in animals treated with viral ILP alone (upper panels, Lu = normal lung, M = metastases). No evidence of microscopic metastatic disease was found in any animal treated with viral ILP and PD-1 blockade (lower panels, Ly = lymphatic nest). * $P \leq 0.05$; **** $P \leq 0.0001$.

Figure 4. Viral ILP and PD-1 blockade transforms the BN175 sarcoma microenvironment. All analyses were performed on tumours collected on Day 12 following treatment. (**A-D**) Flow cytometry analysis (n = 3 animals per group). Viral ILP and PD-1 blockade increased intratumoural $CD3^+$ lymphocytes (**A**), with preferential expansion of $CD8^+$ cytotoxic T cells (**B**) and $CD4^+$ T helper cells (**C**). Viral ILP with or without PD-1 blockade significantly increased expression of granzyme B on T cells (**D**). (**E-I**) Quantification of the density CD8+ infiltration using immunohistochemistry at the invasive margin (**E**) and within the tumour parenchyma (**F**) (n = 6 animals per group). (**G**) Comparison of the density of $CD8^+$ cell infiltration at the invasive margin ('M') and within the tumour parenchyma ('P'). (**H**,**I**) Representative images of $CD8^+$ cell distribution in an untreated tumour (**H**) and following viral ILP + anti-PD-1 antibody (**I**). (**J**) Estimation of the proportion of immune cell subsets following treatment using RNAseq and CIBERSORT (n = 3 animals per group). * $P \leq 0.05$; ** $P \leq 0.01$; *** $P \leq 0.001$; **** $P \leq 0.0001$.

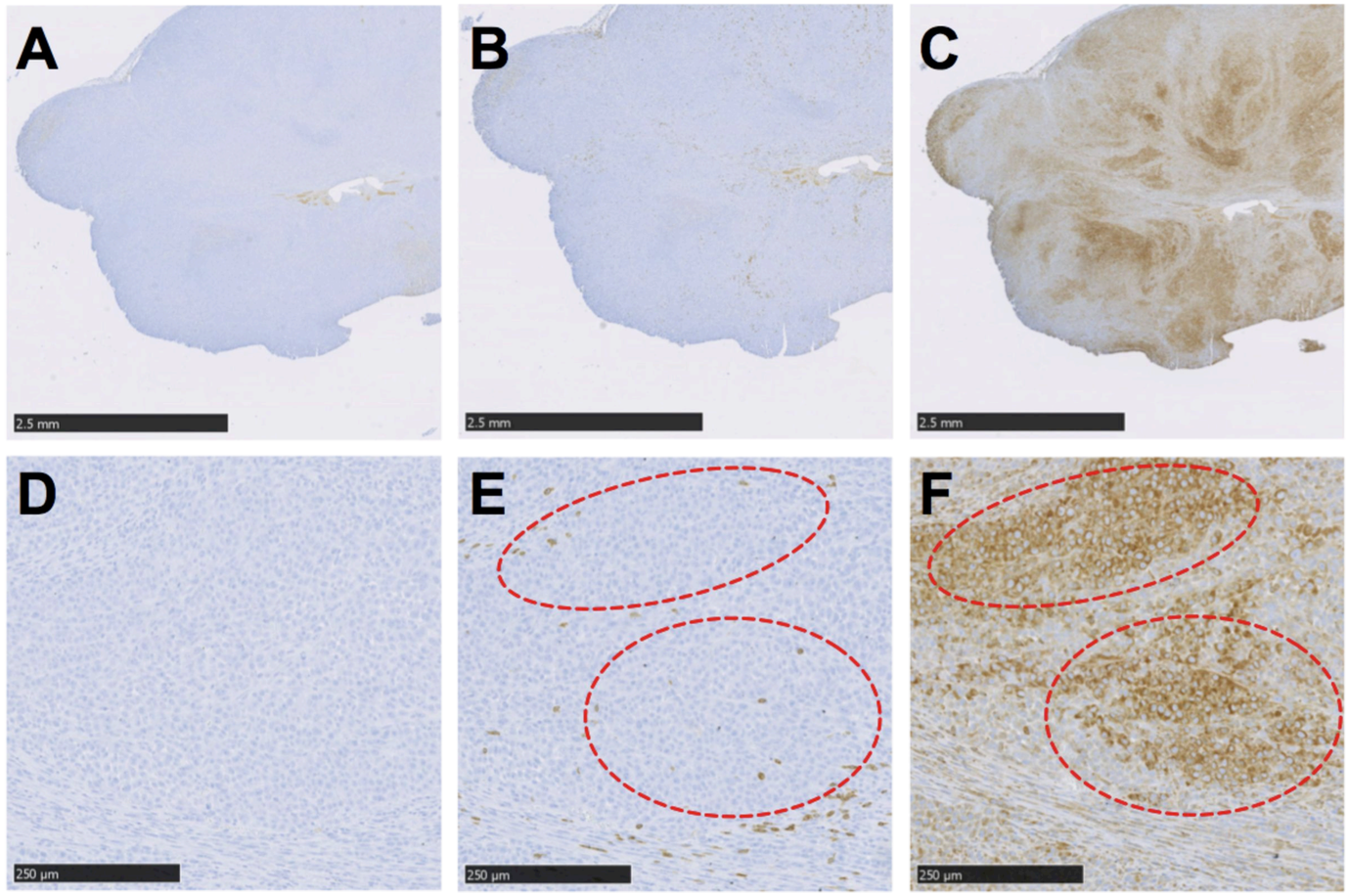

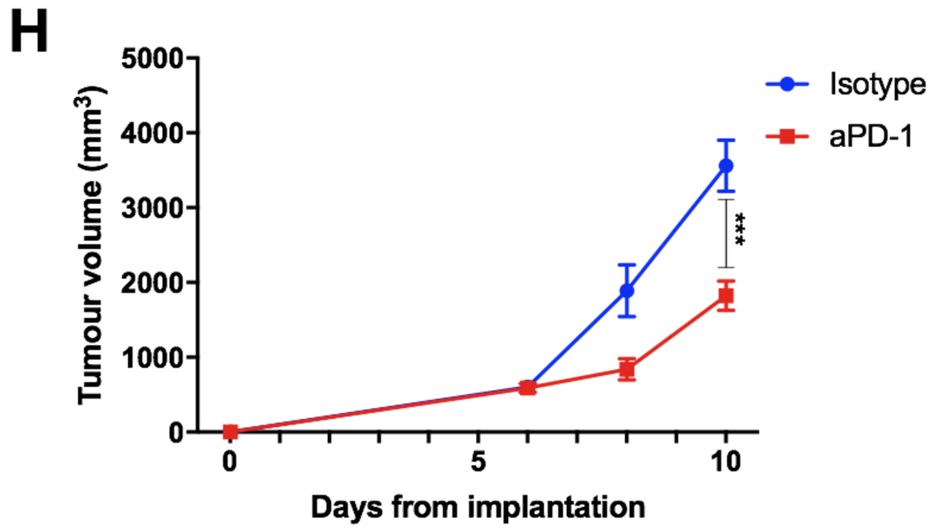

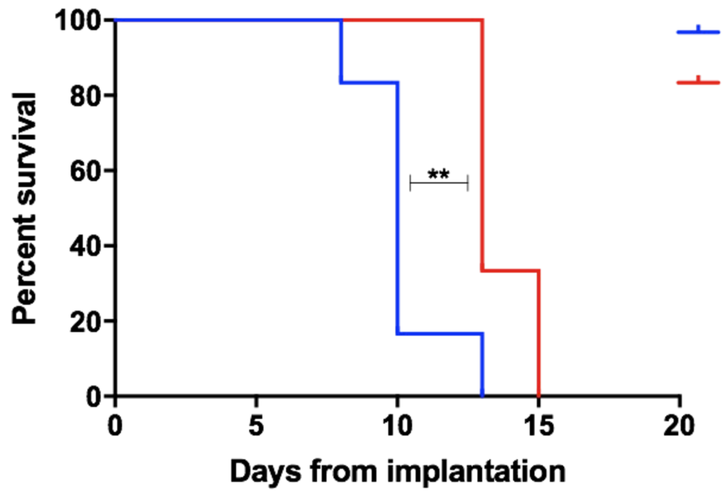

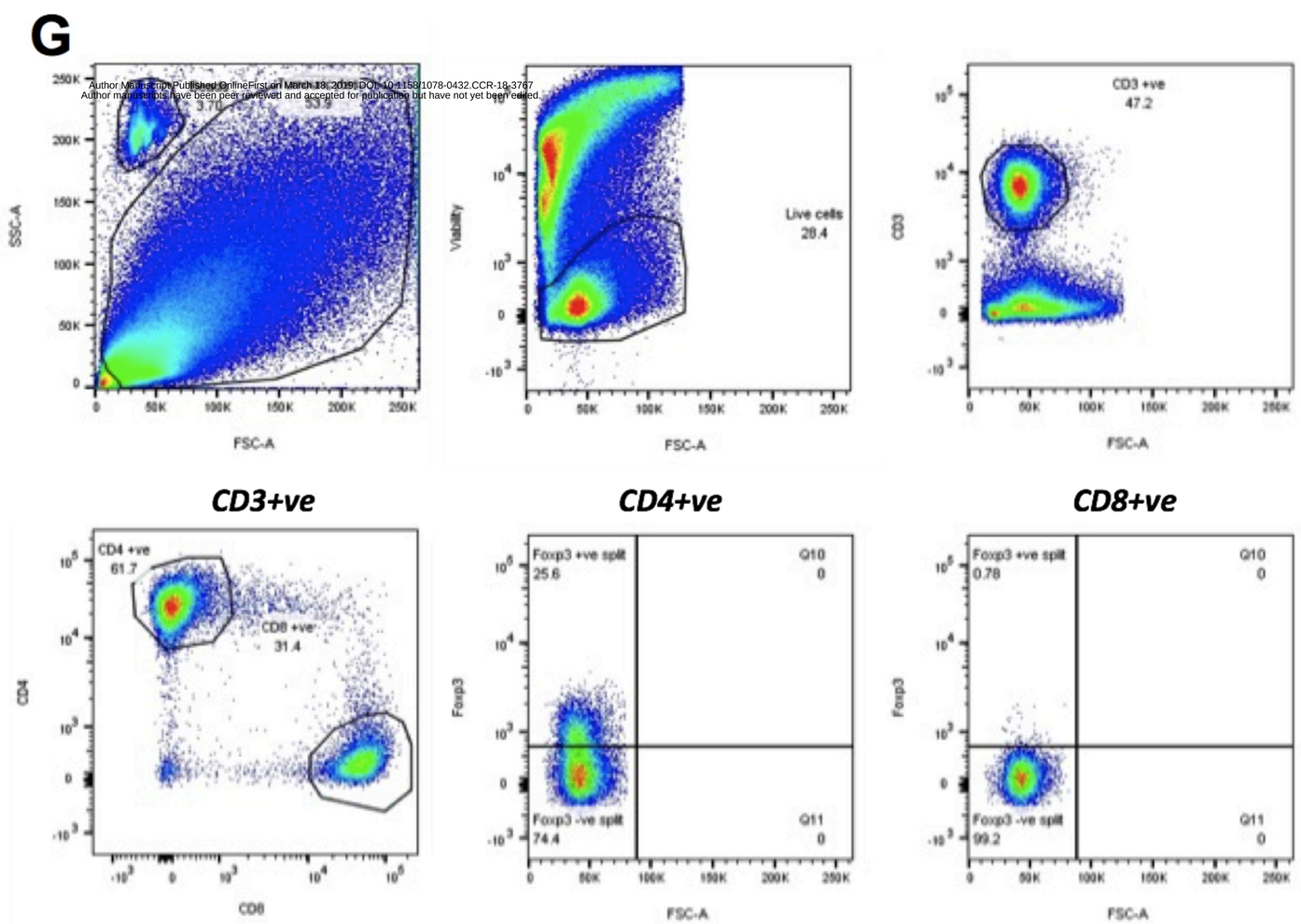

Figure 1

Figure 2

A

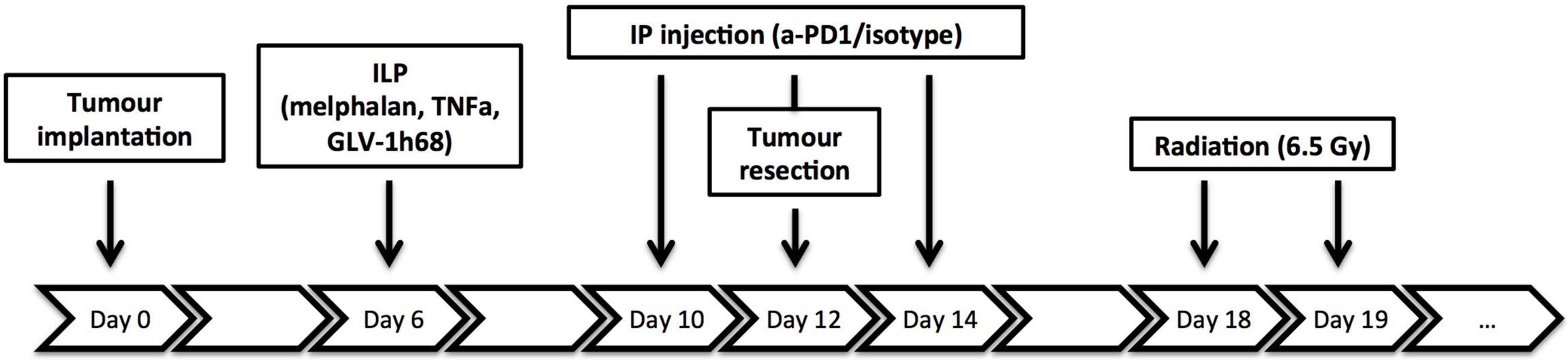

B

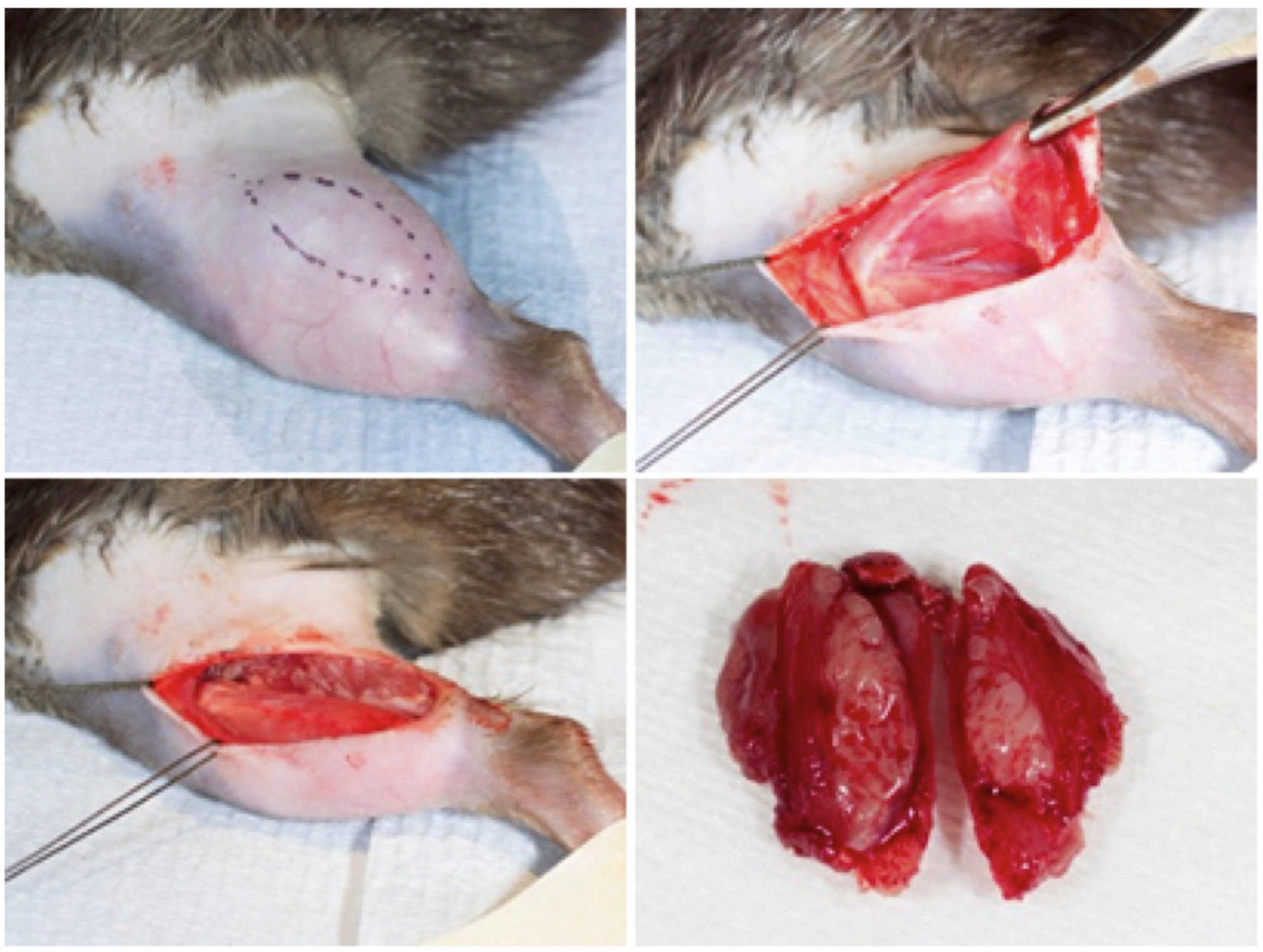

C

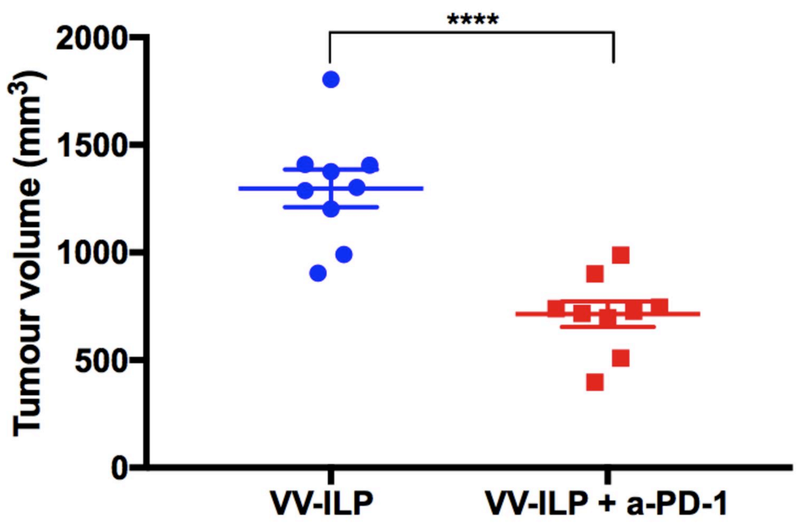

D

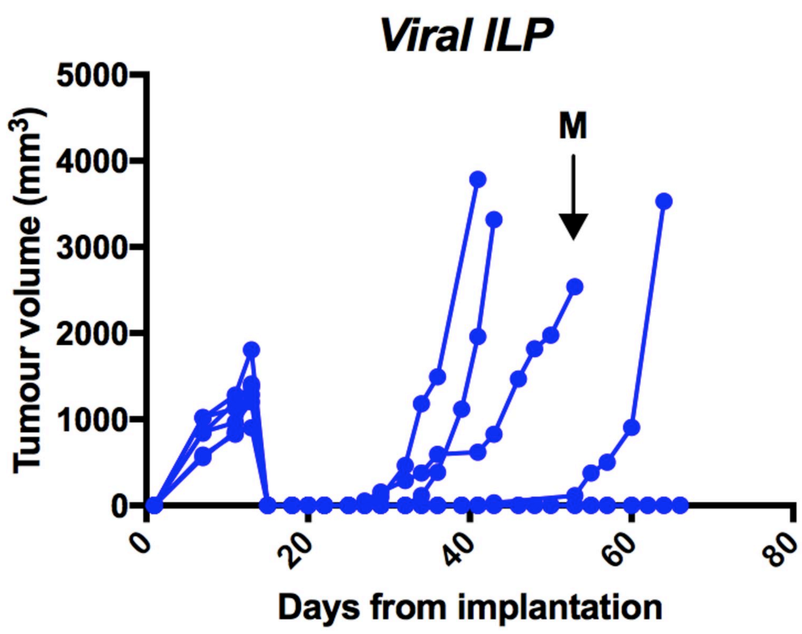

E

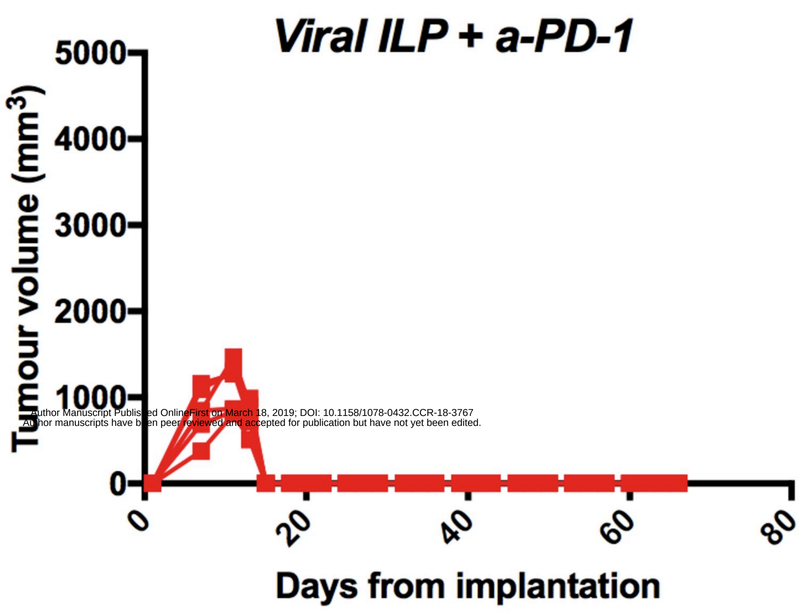

F

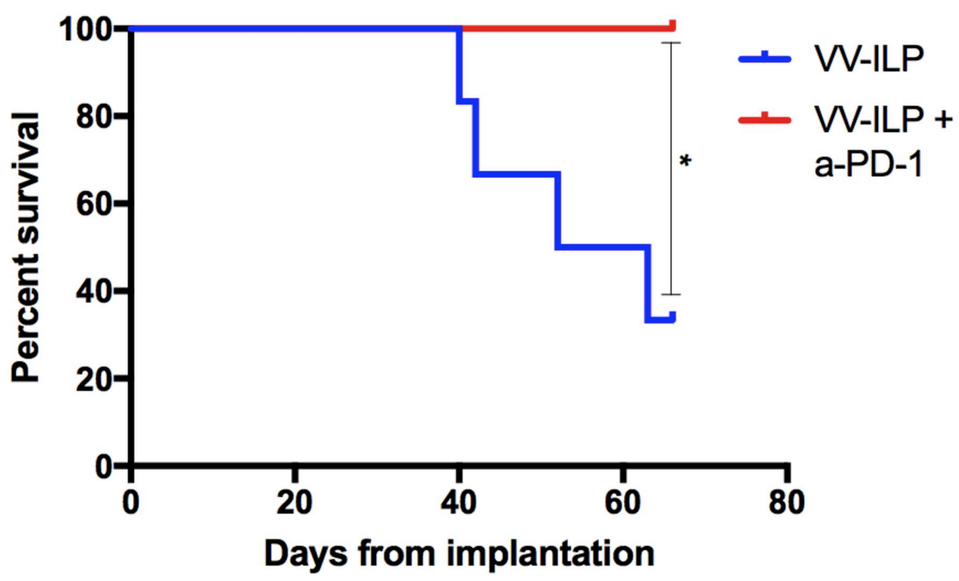

G

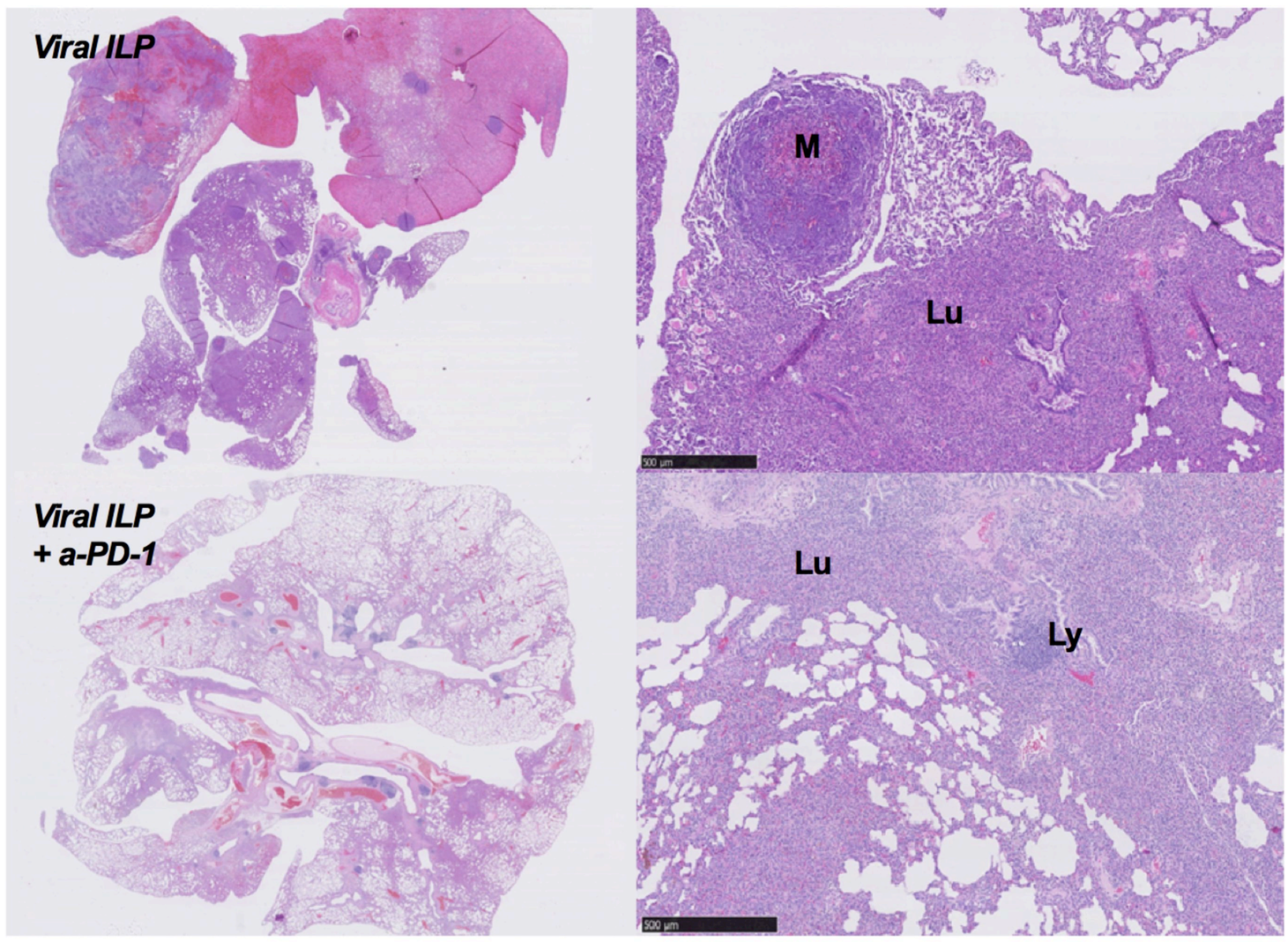

Figure 3

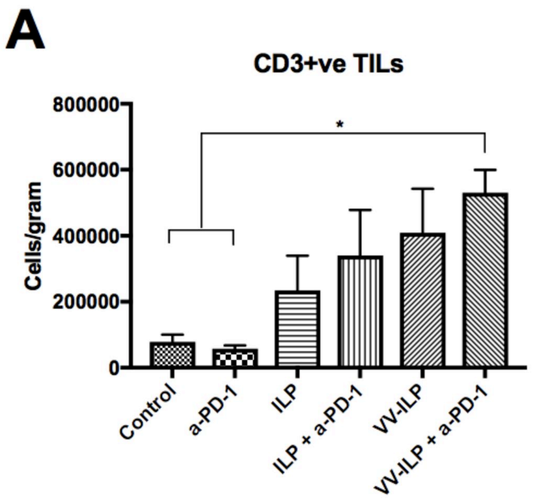

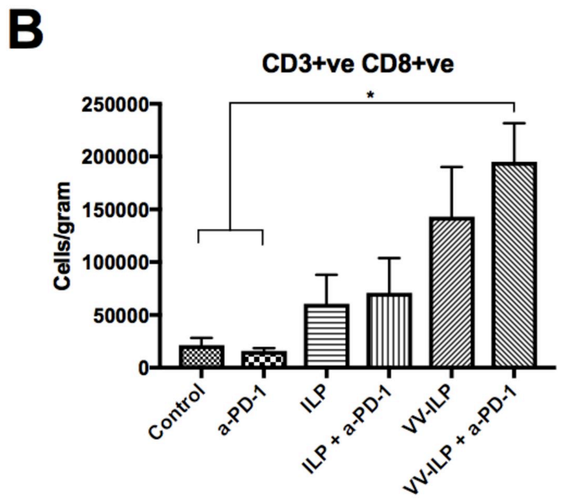

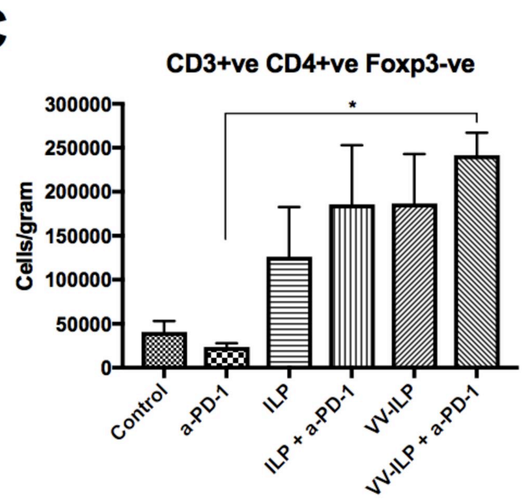

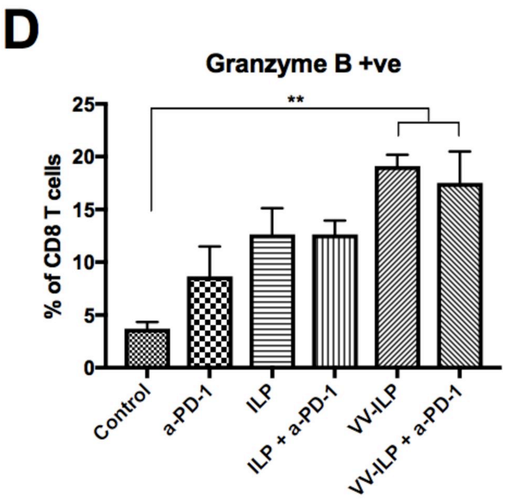

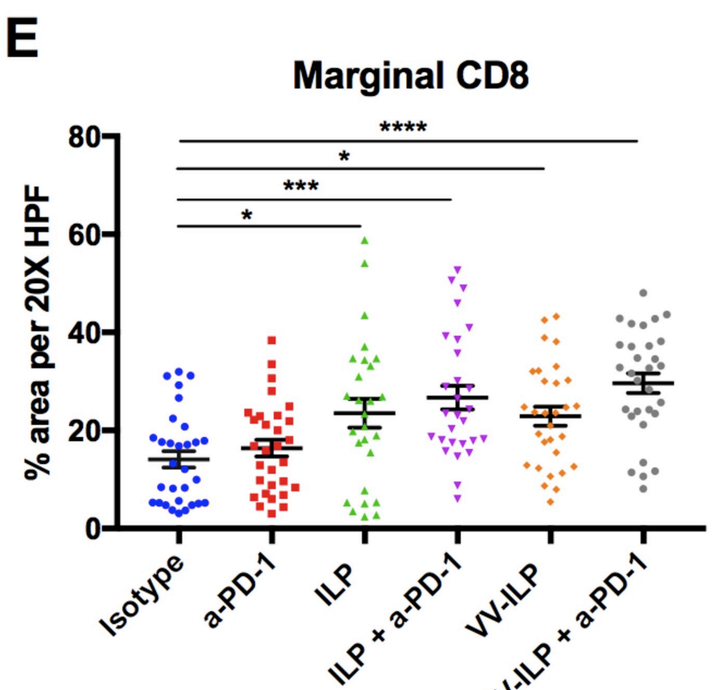

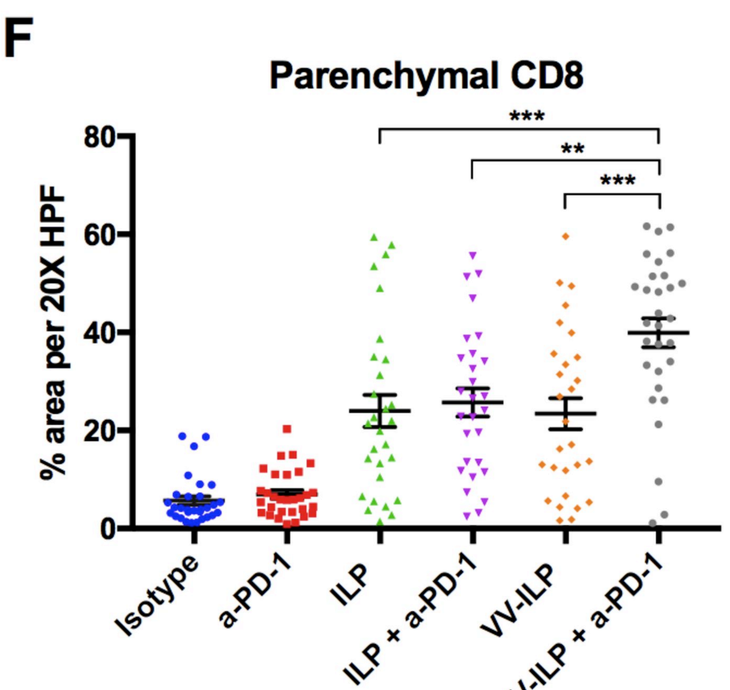

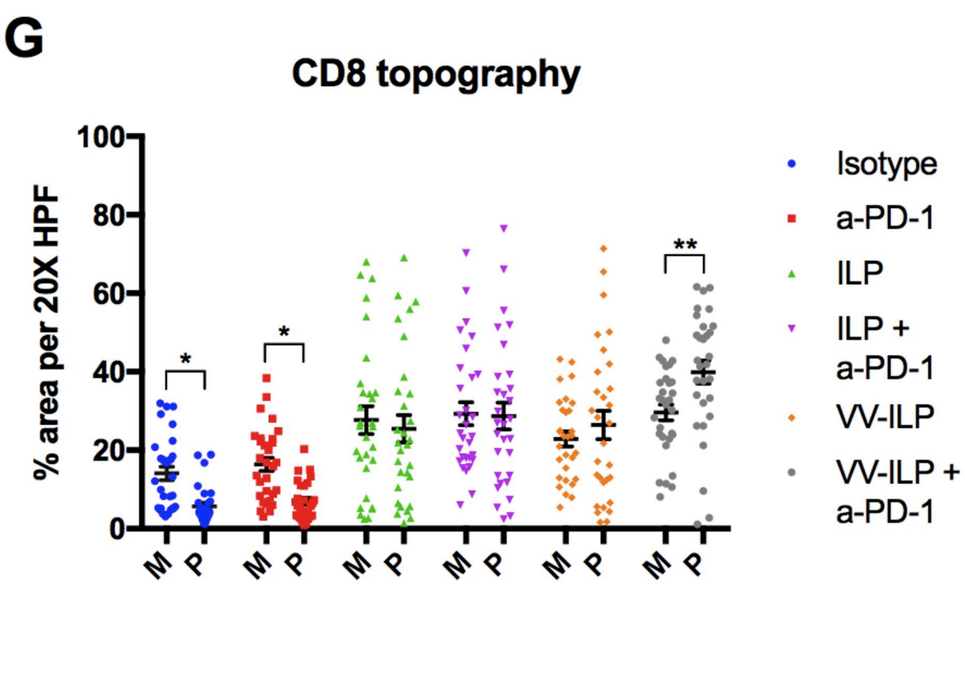

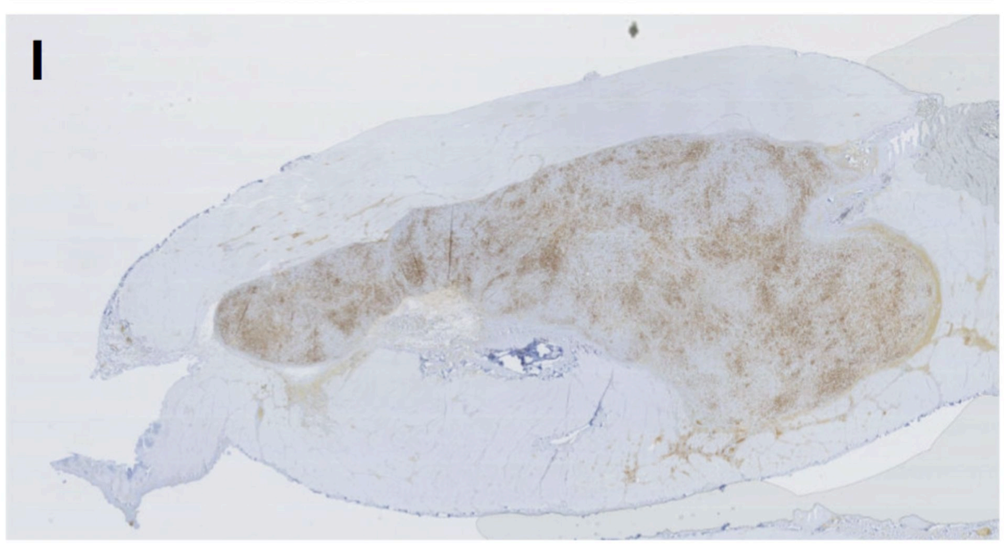

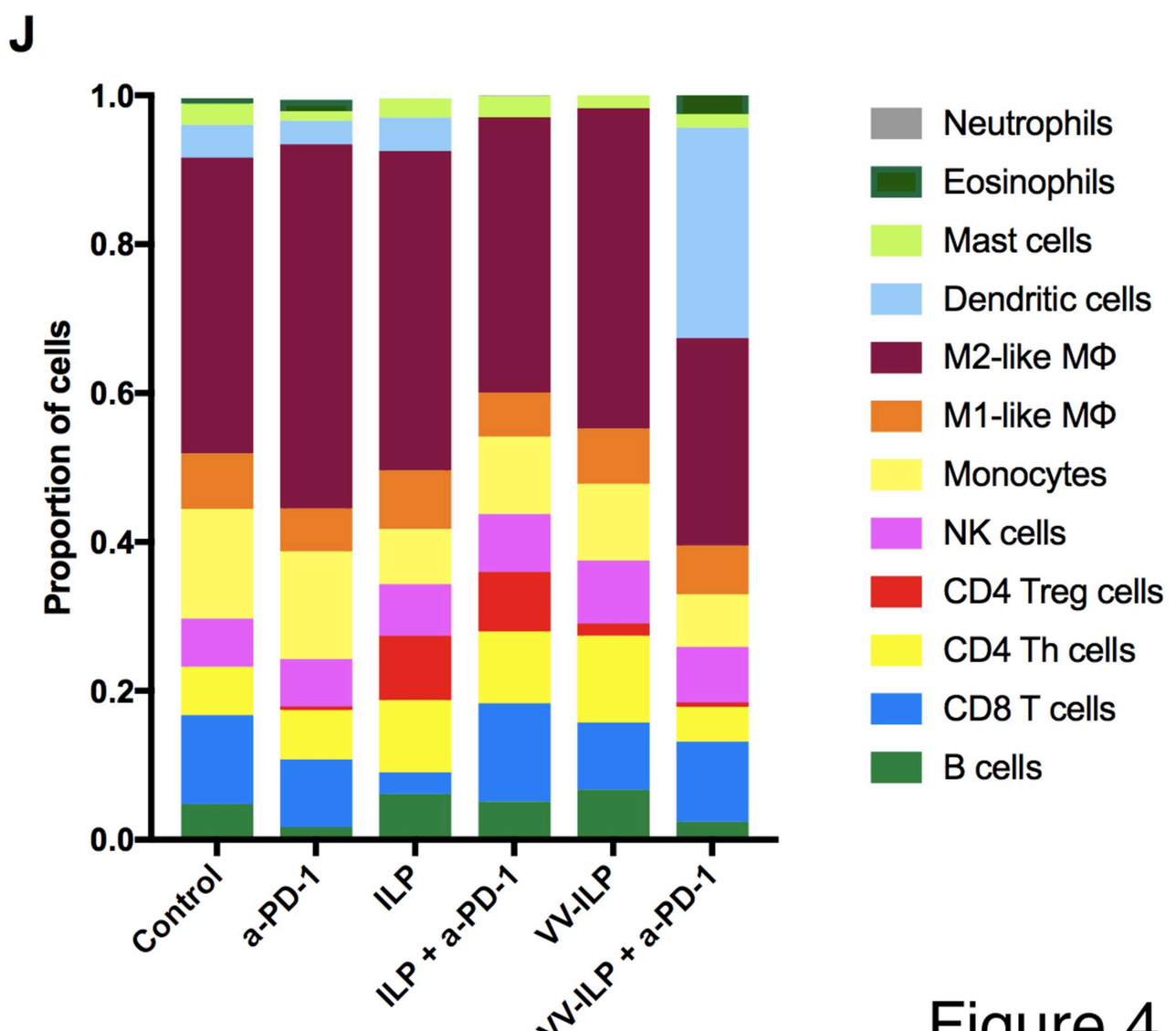

Figure 4

AACR American Association for Cancer Research

Clinical Cancer Research

PD-1 blockade following isolated limb perfusion with vaccinia virus prevents local and distant relapse of soft-tissue sarcoma

Henry G Smith, David Mansfield, Victoria Roulstone, et al.

Clin Cancer Res Published OnlineFirst March 18, 2019.